



# Coupling between Ribotypic and Phenotypic Traits of Protists across Life Cycle Stages and Temperatures

 Songbao Zou,<sup>b,c,d,h</sup> Rao Fu,<sup>b,c,e</sup> Huiwen Deng,<sup>a,g</sup> Qianqian Zhang,<sup>b,c</sup> Eleni Gentekaki,<sup>f</sup>  Jun Gong<sup>a,g</sup>

<sup>a</sup>School of Marine Sciences, Sun Yat-sen University, Zhuhai, China

<sup>b</sup>Yantai Institute of Coastal Zone Research, Chinese Academy of Sciences, Yantai, China

<sup>c</sup>University of Chinese Academy of Sciences, Beijing, China

<sup>d</sup>Key Laboratory of Healthy Freshwater Aquaculture, Ministry of Agriculture and Rural Affairs, Huzhou, China

<sup>e</sup>Shandong Institute of Sericulture, Shandong Academy of Agricultural Sciences, Yantai, China

<sup>f</sup>School of Science, Mae Fah Luang University, Chiang Rai, Thailand

<sup>g</sup>Southern Marine Science and Engineering Guangdong Laboratory, Zhuhai, China

<sup>h</sup>Key Laboratory of Fish Health and Nutrition of Zhejiang Province, Zhejiang Institute of Freshwater Fisheries, Huzhou, China

**ABSTRACT** Relationships between ribotypic and phenotypic traits of protists across life cycle stages remain largely unknown. Herein, we used single cells of two soil and two marine ciliate species to examine phenotypic and ribotypic traits and their relationships across lag, log, plateau, cystic stages and temperatures. We found that *Colpoda inflata* and *Colpoda steinii* demonstrated allometric relationships between 18S ribosomal DNA (rDNA) copy number per cell (CNPC), cell volume (CV), and macronuclear volume across all life cycle stages. Integrating previously reported data of *Euplotes vannus* and *Strombidium sulcatum* indicated taxon-dependent rDNA CNPC-CV functions. Ciliate and prokaryote data analysis revealed that the rRNA CNPC followed a unified power-law function only if the rRNA-deficient resting cysts were not considered. Hence, a theoretical framework was proposed to estimate the relative quantity of resting cysts in the protistan populations with total cellular rDNA and rRNA copy numbers. Using rDNA CNPC was a better predictor of growth rate at a given temperature than rRNA CNPC and CV, suggesting replication of redundant rDNA operons as a key factor that slows cell division. Single-cell high-throughput sequencing and analysis after correcting sequencing errors revealed multiple rDNA and rRNA variants per cell. Both encystment and temperature affected the number of rDNA and rRNA variants in several cases. The divergence of rDNA and rRNA sequence in a single cell ranged from 1% to 10% depending on species. These findings have important implications for inferring cell-based biological traits (e.g., species richness, abundance and biomass, activity, and community structure) of protists using molecular approaches.

**IMPORTANCE** Based on phenotypic traits, traditional surveys usually characterize organismal richness, abundance, biomass, and growth potential to describe diversity, organization, and function of protistan populations and communities. The rRNA gene (rDNA) and its transcripts have been widely used as molecular markers in ecological studies of protists. Nevertheless, the manner in which these molecules relate to cellular (organismal) and physiological traits remains poorly understood, which could lead to misinterpretations of protistan diversity and ecology. The current research highlights the dynamic nature of cellular rDNA and rRNA contents, which tightly couple with multiple phenotypic traits in ciliated protists. We demonstrate that quantity of resting cysts and maximum growth rate of a population can be theoretically estimated using ribotypic trait-based models. The intraindividual sequence polymorphisms of rDNA and rRNA can be influenced by encystment and temperature, which should be considered when interpreting species-level diversity and community structure of microbial eukaryotes.

**KEYWORDS** cell size, copy number variation, growth rate, life cycle, warming

**Citation** Zou S, Fu R, Deng H, Zhang Q, Gentekaki E, Gong J. 2021. Coupling between ribotypic and phenotypic traits of protists across life cycle stages and temperatures. *Microbiol Spectr* 9:e01738-21. <https://doi.org/10.1128/Spectrum.01738-21>.

**Editor** Jeffrey A. Gralnick, University of Minnesota

**Copyright** © 2021 Zou et al. This is an open-access article distributed under the terms of the [Creative Commons Attribution 4.0 International license](https://creativecommons.org/licenses/by/4.0/).

Address correspondence to Jun Gong, gongj27@mail.sysu.edu.cn.

**Received** 7 October 2021

**Accepted** 16 October 2021

**Published** 24 November 2021

Protists are single-celled eukaryotes of astounding morphological and functional diversity inhabiting virtually every life-harboring niche on this planet. These microorganisms have complex life cycles comprising stages of distinct phenotypic traits (e.g., morphology, cell size, cystic/vegetative status, and growth rate), which undergo changes in response to fluctuating environmental variables (1–6). Recently, the advent of sequencing technologies has greatly facilitated the study of ribotypic traits, i.e., the qualitative and quantitative attributes of rRNA genes (ribosomal DNA [rDNA]) and/or rRNA transcripts, which are used to assess protistan diversity and community composition in natural ecosystems (7).

The rDNA copy number (CN) and its dynamics provide important information on the diversity and quantity of protistan cells in molecular ecological studies. The eukaryotic rDNA comprises encoding regions for 18S, 5.8S, and 28S rRNA, noncoding internal transcribed regions (ITS1 and ITS2) and intergenic spacers and is generally arranged in tandem arrays of multiple copies. The transcribed 18S rRNA is the structural RNA for the small subunit of eukaryotic cytoplasmic ribosomes, which are the sites of protein synthesis and thus closely tied to cellular growth and development (8). Recently, variations in per-cell rDNA and rRNA CNs have been linked to phenotypic traits, such as cell volume (CV) and growth rate of exponentially growing ciliated protists (9). The dynamic nature of rDNA CN across life cycle stages has also been demonstrated in a foraminiferan species (10). Nevertheless, the association(s) between ribotypic and phenotypic traits in protists remains little explored. Moreover, the quantitative relations, if any, between ribotypic and phenotypic traits across different growth stages (e.g., lag, log, plateau, and cystic phases) have yet to be investigated.

Cysts are dormant forms comprising essential life cycle stages for many protistan taxa exposed to unfavorable conditions (1, 11, 12). However, rDNA CN data of cysts are only available for a limited number of protistan species (13, 14), and CN of rRNA in a cyst has seldomly been quantified, probably due to the common assumption that rDNA is sparsely or not at all transcribed in the dormant stages. The rRNA/rDNA CN ratio has been used as an indicator of microbial activity/dormancy; however, this approach is not entirely problem free (9, 15). Experimental data of rRNA and rDNA CNs for different types of cysts are lacking. These can be used to build suitable models in order to properly estimate dormancy in environmental samples.

The rDNA operons of diverse protistan groups have a high degree of intraindividual sequence polymorphisms (16–21). During the life cycle of a protistan cell (10), and in response to changing temperatures (9), cellular rDNA copies are gained or lost. However, little is known about whether specific rDNA sequence variants are selected at different life cycle stages or under varying conditions. Similarly, the dynamics of rRNA sequence variants under these conditions warrant further investigation, as selective transcription of specific rDNA operons has been previously shown for several prokaryotes and a parasitic protist (22–25).

Ciliates comprise one of the most intensely studied groups of protists, making them ideal models for examining links between ribotypic and phenotypic traits across life history stages. Ciliate species have two morphologically and functionally distinct nuclei, a polyploid somatic macronucleus and one or several diploid germ line micronuclei. The macronucleus contains hundreds to thousands of transcriptionally active nanochromosomes that function in all cellular events. The micronucleus is transcriptionally silent during cell growth, but following sexual reproduction, it gives rise to the macronucleus (26). The latter contains numerous nucleoli, the sites of rDNA sequences, rRNA synthesis, and ribosome subunit assembly (27). During encystment and excystment, the number and size of nucleoli varies, accompanying loss and gain of macronuclear DNA (28, 29). This raises the question of whether in ciliates cellular ribotypic CNs are more related to macronuclear size than to CV across life cycle stages.

*Colpoda* has long been used as a model for the study of cyst-related biology and ecology (28, 30, 31). In this work, we used two ubiquitously distributed soil ciliate species of *Colpoda* to investigate both rDNA and rRNA CNs across lag, log (exponential), plateau (stationary), unstable, and resting cyst stages. The rDNA copies quantified and sequenced in this study were considered to be of macronuclear origin. Their phenotypic features (cell size, macronuclear size, nucleocytoplasmic ratio, and maximum growth rate) were determined

for cells reared at two temperatures. Temperature as a key environmental factor was investigated because of its importance in many aspects, including climate change, effect on biochemical kinetics, metabolic and physiological processes, and modulation of body size and growth rate (32). The temperature and growth stage relationships to intraindividual polymorphisms of ribotypic sequences were explored. We also extended previous work on the marine ciliates *Euplotes vannus* and *Strombidium sulcatum*, which were reared at three different temperatures by analyzing rDNA and rRNA sequence diversity in actively growing cells (9). Our main expectations were as follows: (i) the scaling relationships between rDNA and rRNA transcript CNs and phenotypic traits (CV and macronuclear size) would generally hold across life cycle stages including resting cysts, and (ii) the variant richness and composition of intraindividual rDNA and rRNA molecules would be life stage and temperature dependent.

## RESULTS

**Cell volume, macronuclear volume, and nucleocytoplasmic ratio.** The lag, log, plateau, and resting cyst phases of *Colpoda steinii* and *Colpoda inflata* were distinguishable when cultured under replete bacterial prey conditions at both 18°C and 28°C (Fig. 1A). At 28°C, the two species grew approximately 2 and 6 times faster than at the 18°C treatments, respectively. At both temperatures, the smaller species (*C. steinii*) grew consistently faster than the larger one (*C. inflata*) as follows:  $7.2 \pm 0.87 \text{ d}^{-1}$  (mean  $\pm$  standard error [SE]) versus  $5.1 \pm 0.09 \text{ d}^{-1}$  at 28°C, and  $3.6 \pm 0.32 \text{ d}^{-1}$  versus  $0.9 \pm 0.32 \text{ d}^{-1}$  at 18°C (Fig. 1B). Abundant unstable cysts were successfully obtained by chilling actively growing cells of *C. steinii* at 0°C for 4 h and *C. inflata* at 4°C for 10 h (see Fig. S3 in the supplemental material).

The cell volume (CV) of both *Colpoda* species was progressively reduced through lag, log, and plateau to resting cyst phases at both temperatures (Fig. 1C and D and Fig. 2A). In the 18°C treatment of *C. inflata*, the largest CV (about  $2.14 \times 10^5 \mu\text{m}^3$ ) was recorded at the lag phase. Upon entering the exponential phase, cells became smaller and further shrank by 46% during the plateau phase. Relative to the log-phase cells, the resting cysts of this species were greatly reduced in size by 83%. *Colpoda inflata* cells were significantly smaller in the 28°C versus the 18°C treatment ( $P < 0.05$  in all cases) (Fig. 2A). Compared to the log-phase cells, the CV of the small-sized *C. steinii* was reduced by 85% and 69% during encystment at 18°C and 28°C treatments, respectively. At any given phase, the CV was always larger in the cultures reared at 18°C rather than at 28°C ( $P < 0.05$ ), except for the resting cysts, whose size (about  $2.0 \times 10^3 \mu\text{m}^3$ ) was not significantly different between these two temperature treatments (Fig. 2A).

The unstable cysts of both *Colpoda* species were generally larger than the resting cysts but smaller than the plateau-phase cells (Fig. 2A). At 18°C, the volumes of unstable cysts of *C. steinii* and *C. inflata* were on average  $5.3 \times 10^3$  and  $0.21 \times 10^5 \mu\text{m}^3$ , respectively (Fig. 1C and Fig. 2A). A similar pattern of unstable cyst size was observed at 28°C (Fig. 2A). Assuming a globular body shape for *C. steinii* and *C. inflata* cells, the equivalent spherical diameter (ESD) of the cells ranged from 13 to 29  $\mu\text{m}$  and from 25 to 74  $\mu\text{m}$ , respectively, with cross-phase patterns similar to those of CV (Fig. 2B).

Macronuclear volume (MV) exhibited a similar trend to the CV in both *Colpoda* species, i.e., decreasing gradually through lag, log, and plateau phases to resting cyst, regardless of cultivation temperatures (Fig. 2C). *Colpoda inflata* had a consistently larger MV than *C. steinii* at any given phase ( $P < 0.05$ ). For both species, when the MV was relatively smaller (e.g.,  $\text{MV} < 500 \mu\text{m}^3$  or macronuclear diameter  $< 10 \mu\text{m}$ ), it was consistently and significantly reduced in the 18°C treatments relative to the 28°C treatments. However, when the macronucleus was larger (i.e., macronuclear diameter  $> 10 \mu\text{m}$ ), the effect of temperature increase on MV was insignificant ( $P > 0.05$ ) (Fig. 2C).

The nucleocytoplasmic ratio of two *Colpoda* species ranged from approximately 1% to 8% and tended to progressively increase from lag and log to plateau phases and resting cysts (Fig. 2D). The log-phase cells of *C. steinii* had the lowest nucleocytoplasmic ratios (on average 2.92% to 2.61% at 18°C and 28°C, respectively), which were 1.13 to 1.32 times lower than those in lag and plateau phases, respectively. Culturing at the higher temperature generally did not induce significant decreases in the nucleocytoplasmic ratio in most growth

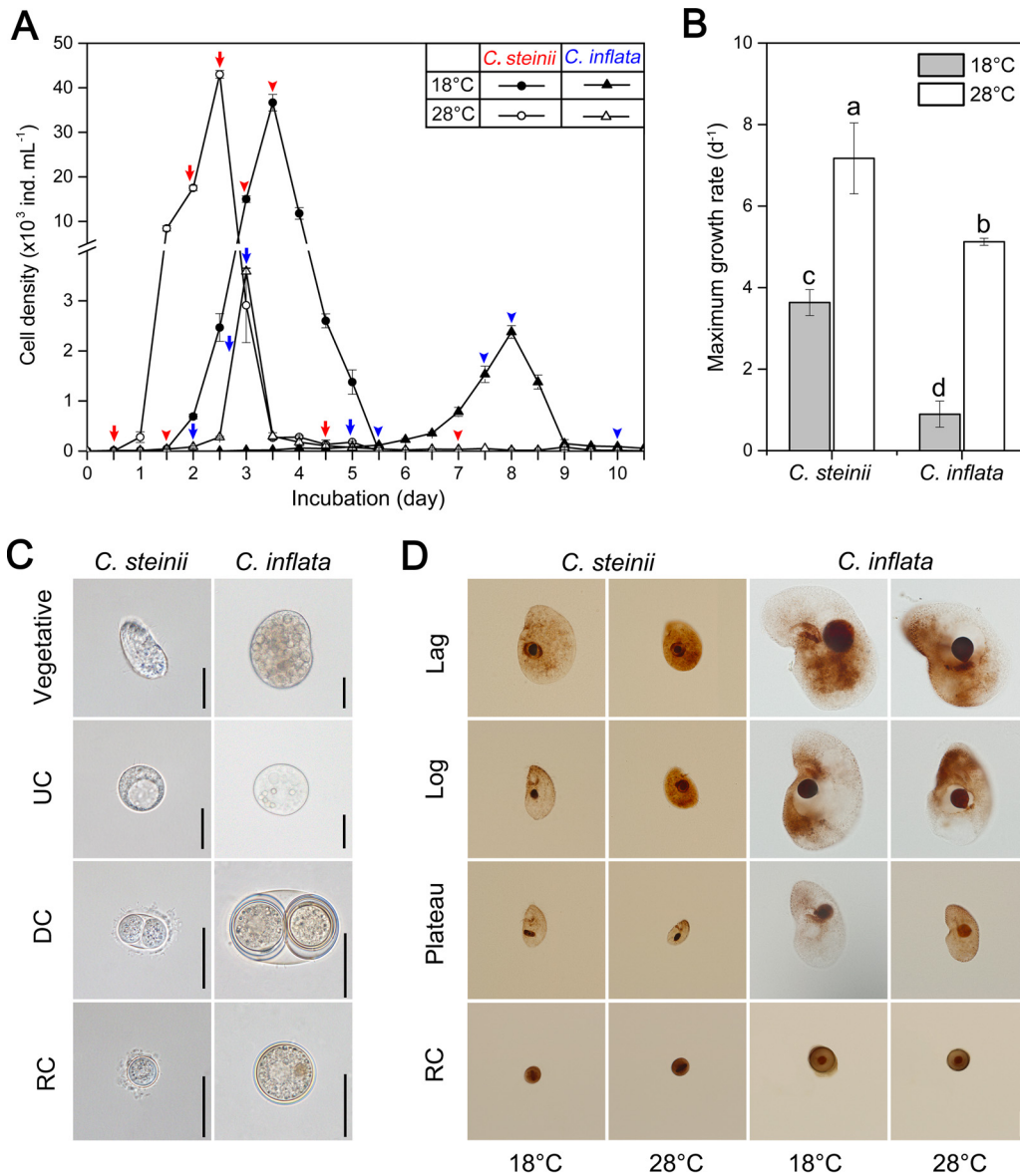


**FIG 1** Growth and morphology of the soil ciliates *Colpoda steinii* and *C. inflata* reared at 18°C and 28°C. (A) Growth curves of *C. steinii* (arrows and arrowheads in red) and *C. inflata* (arrows and arrowheads in blue) depicting cell isolation time points at lag, log, plateau, and resting cyst phases. (B) Maximum growth rates of cells at log phase. Treatments not sharing common letters indicate significant differences ( $P < 0.05$ ). (C) Morphology of vegetative cells, unstable cysts (UC), dividing cysts (DC), and resting cysts (RC) from life. (D) Microphotographs of fixed specimens after protargol impregnation. Cell and macronuclear sizes across life cycle stages, temperatures, and species. Scale bars = 20  $\mu\text{m}$ .

phases of either species ( $P > 0.05$ ), except for resting cysts of *C. steinii*, which had a much higher nucleocytoplasmic ratio (on average 7.93%) at 18°C than that at 28°C (3.82%). Compared with the small species, *Colpoda inflata* usually had lower cytoplasmic volume ratios in all phases and at both temperatures (Fig. 2D). Regression analysis showed that macronuclear volume scaled well with  $CV^{0.83}$ , and the nucleocytoplasmic ratio fit well to a power-lower function of  $ESD^{-0.522}$  (Fig. 2E and F).

**Variations in single-cell rDNA and rRNA copy numbers.** The per-cell rDNA and rRNA copy numbers varied significantly among growth phases (analysis of variance [ANOVA],  $P < 0.001$ ), showing a consistently decreasing trend from the lag, log, and plateau phases to the resting cyst stage for both *Colpoda* species and at both temperatures. The resting cysts of both *Colpoda* species lost ~50% to ~90% of rDNA and over ~89% to ~99.99% of rRNA copies relatively to the cells in log phase (Fig. 3A and B).

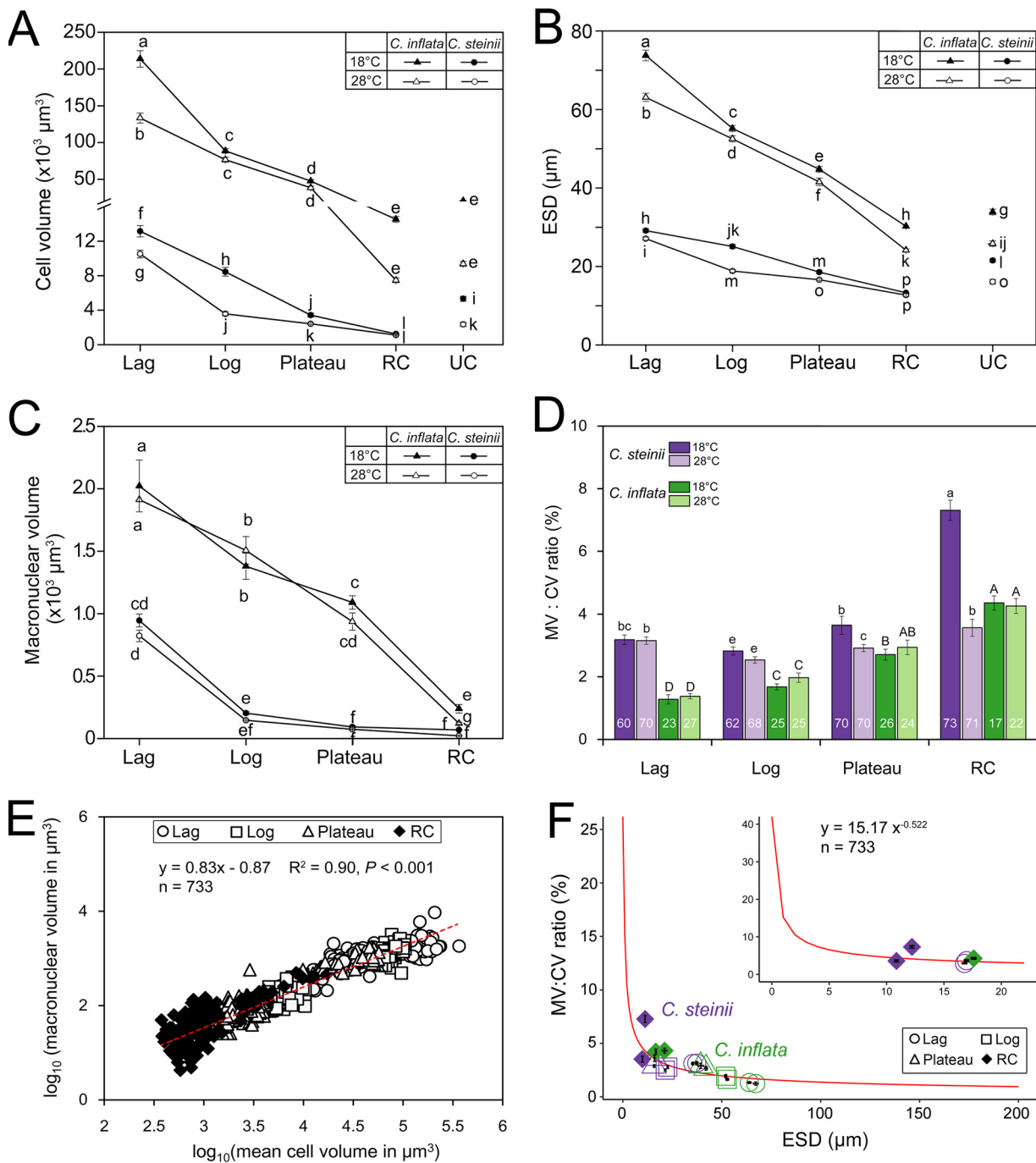


**FIG 2** Variation in phenotypic traits of *Colpoda steinii* and *C. inflata* across life cycle stages and at two temperatures. Unconnected points in line graph panels indicate unstable cysts. (A) Cell volume progressively decreased from lag to resting cyst phases. In general, unstable cysts were larger than resting cysts. Cells at a given growth phase were consistently larger at 18°C than at 28°C. (B) Equivalent spherical diameter (ESD) progressively decreased from lag to resting cyst phases. (C) Macronuclear volume changed similarly to cell volume across stages but was mostly not significant between the two temperatures. (D) Ratio of macronuclear to cell volume (MV/CV) across life cycle stages. Numbers in the bars indicate the numbers of cells counted. (E) A linear log-log relationship between macronuclear (MV) and cell volumes (CV) across life cycle stages (lag, log, plateau, and RC). (F) A modeled scaling relationship between MV/CV ratio and equivalent spherical diameter (ESD). Nucleocytoplasmic ratio varies dramatically in small cells (e.g., pico- [ $< 2 \mu\text{m}$ ] and nano-sized protists [ $\sim 2$  to  $\sim 20 \mu\text{m}$ ]) but changes only slightly in large cells (e.g., microplanktons [ $\sim 20$  to  $\sim 200 \mu\text{m}$ ]). Not sharing common letters indicates significant differences ( $P < 0.05$ ). RC, resting cyst; UC, unstable cyst.

The rDNA amount was reduced greatly in the resting cysts of this species at 18°C to about 1,000 copies per cyst (Fig. 3A). Although the unstable cysts of *C. steinii* were smaller than the plateau-phase cells, the two had a similar copy number of rDNA ( $[2.0 \pm 0.2] \times 10^3$ ). Compared with the lower temperature treatments, *C. steinii* cultured at

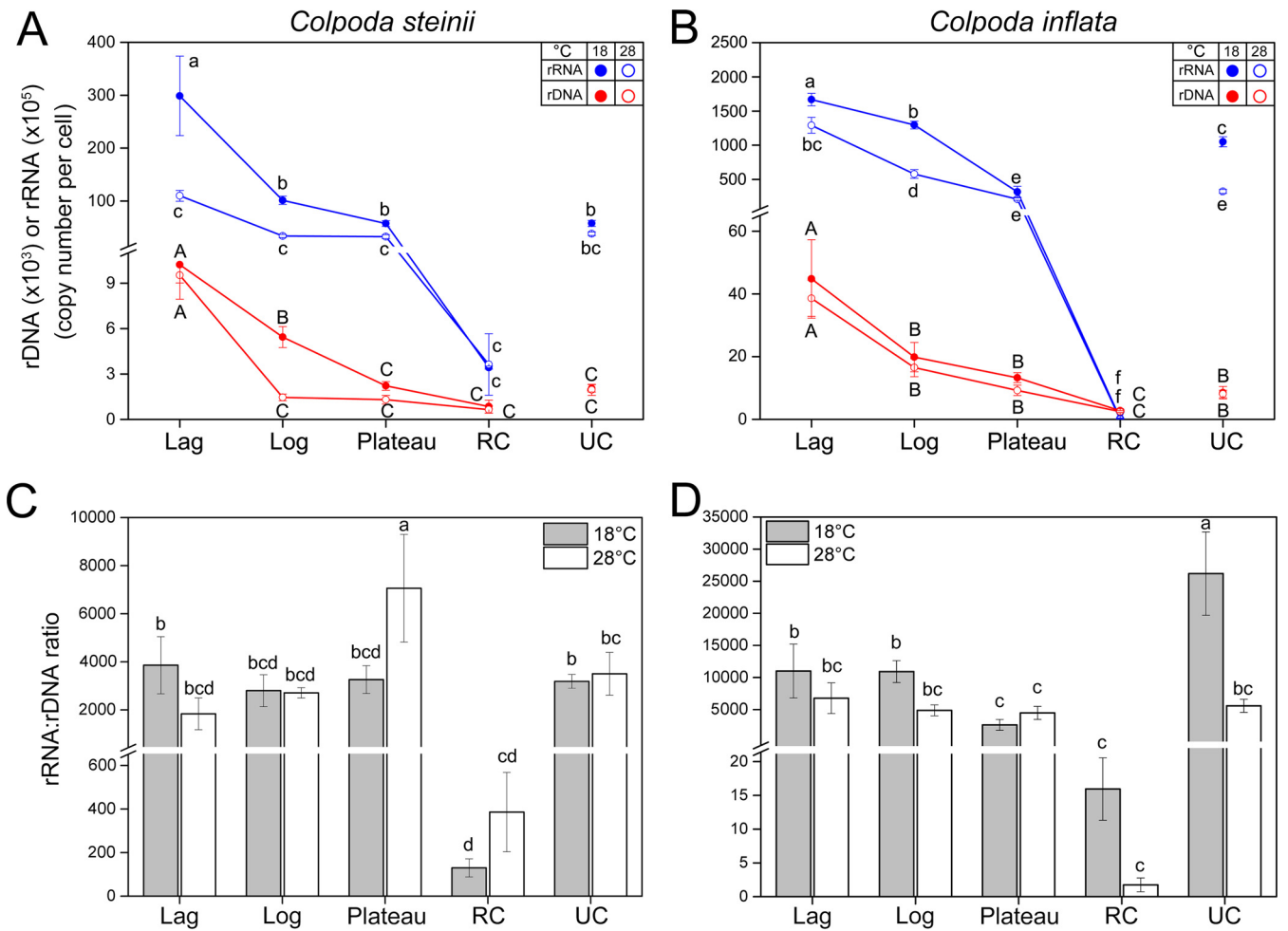


**FIG 3** Variation in ribotypic traits of *Colpoda steinii* (A and C) and *C. inflata* (B and D) across lag, log, plateau, resting (RC), and unstable cyst (UC) stages and at two culturing temperatures. Unconnected points in line graph panels indicate unstable cysts. (A, B) Single-cell 18S rDNA and rRNA copy numbers progressively and significantly decreased from lag to RC phase. Cells in the UC stage generally had similar amounts of rDNA and rRNA as the vegetative cells in plateau phase. (C, D) Copy number ratios of rRNA to rDNA in single cells were significantly lower in resting cysts of both species. The ratio was consistent in all other life cycle phases of *C. steinii* and lower in plateau and unstable cystic phases of *C. inflata* (relative to its log phase). Bars represent standard errors. Treatments not sharing common letters indicate significant differences ( $P < 0.05$ ).

28°C had lower per-cell rDNA copy numbers, particularly for the cells at log and plateau phases ( $P < 0.05$ ).

The large-sized *Colpoda* species had many more rDNA copies than the small-sized congener across all life cycle stages (e.g.,  $1.98 \times 10^4$  versus  $5.4 \times 10^3$  at log phase) (Fig. 3B). Phase-specific comparisons showed that warming had no significant effect in modulating per-cell rDNA content in this species ( $P > 0.05$ ). The resting and unstable cysts of *C. inflata* contained about 2,500 and 8,100 rDNA copies, respectively, which were about 3.3 and 4.2 times higher than those of *C. steinii* (Fig. 3B).

The cellular rRNA copies were far more abundant and varied more dramatically across growth stages than the rDNA copies in both *Colpoda* spp. (Fig. 3A and B). In the 18°C treatment, a single cell of *C. steinii* had  $3.0 \times 10^7$ ,  $1.0 \times 10^7$ ,  $5.7 \times 10^6$ , and  $3.4 \times 10^4$  rRNA copies at the lag, log, plateau, and resting cyst stages, respectively (Fig. 3A). At the same temperature, the rRNA molecules were much more abundant in *C. inflata*, with  $1.7 \times 10^8$ ,  $1.3 \times 10^8$ ,  $3.2 \times 10^7$ , and  $3.1 \times 10^4$  copies across these phases (Fig. 3B). Although smaller than the plateau-phase cells, the unstable cysts had relatively similar (in *C. steinii*) or even higher number of rRNA copies (in *C. inflata*) (Fig. 3A and B). Comparing the two temperature treatments, warming always led to a significant decrease in cellular rRNA amount of both species and across all stages plus unstable cysts ( $P < 0.05$ ). A cell at any vegetative growth phase of these two species had approximately 200 to 5,000 times more rRNA copies than resting cysts (Fig. 3A and B).

Differences between the two *Colpoda* species in terms of the patterns of rRNA/rDNA CN ratio across growth phases and between temperature treatments were minor (Fig. 3C and D). The rRNA/rDNA CN ratios in *C. steinii* ranged from 2,000 to 4,000, without statistical differences among the lag, log, plateau, and unstable cystic stages ( $P > 0.05$ ) (Fig. 3C). Nevertheless, at 18°C the rRNA/rDNA ratios in *C. inflata* decreased from 10,000 to 2,000 when population growth entered the plateau phase; the rRNA/rDNA ratio of unstable cysts was also significantly high in the 18°C treatment in this species (Fig. 3D). Furthermore, while the rRNA/rDNA ratios in log-phase cells, unstable, and resting cysts of *C. inflata* significantly dropped at the higher culturing temperature (Fig. 3D), the same was not observed in *C. steinii* (Fig. 3C). Nevertheless, the resting cysts of both species had much lower rRNA/rDNA ratios (150 to 400 in *C. steinii* and 2 to 16 in *C. inflata*) than the cells in all other phases (Fig. 3C and D).

**Linking ribotypic with phenotypic traits.** Based on all CN data of vegetative and cystic cells of these two *Colpoda* spp., correlation and linear regression analyses showed that both rDNA ( $rDNA_{\text{CNPC}}$ ) and rRNA copy number per cell ( $rRNA_{\text{CNPC}}$ ) were positively and significantly related to CV or ESD and could fit well to linear regression curves ( $R^2 = 0.91$ ;  $P < 0.01$ ) (Fig. 4A; Table 1, equation numbers 1 and 2), irrespective of cell cycle stage.

For an idealized population of similar cell size, the total rDNA copy number of the population ( $rDNA_{\text{total}}$  or  $N \cdot rDNA_{\text{CNPC}}$ ) can be expressed as a function of ESD and abundance of the cells ( $N$ ) (Table 1, equation number 3). Since  $N \cdot rDNA_{\text{CNPC}}$  can be experimentally determined (for example, by using quantitative PCR [qPCR]), this equation indicates that inferring cell abundance of a population using rDNA copy numbers depends on cell size of the population.

The correlation between  $rRNA_{\text{CNPC}}$  and CV across all life cycle phases including resting cysts (+RC) was significant ( $P = 0.005$ ) (Table 1, equation number 4). However, the  $R^2$  score (37%) was only moderate (Fig. 4A). Nevertheless, when the rRNA CN data of the resting cysts (which contained an extremely low rRNA amount that could not be easily predicted when using cell size, i.e., the four blue full diamonds that are discrete from other points in Fig. 4A) were excluded from the analysis (−RC), the relationship became well supported ( $R^2 = 0.84$ ) (Table 1, equation number 5). Similarly, the total rRNA copy number of the population ( $rRNA_{\text{total}}$  or  $N \cdot rDNA_{\text{CNPC}}$ ) can be expressed as a function of ESD and cell abundance ( $N$ ) (Table 1, equation number 6). Based on a combination of equation numbers 3 and 6 in Table 1, which presume all cells in a population are nonresting cysts, the copy number ratio of total rRNA/rDNA depends on a single factor, ESD or cell size (Table 1, equation number 7). The correlations between MV of cells at all life cycle stages and ribotype CNs exhibited patterns similar to the ones observed for CV (see Table 1, equation numbers 8 to 10; see also Fig. S4 in the supplemental material).

Assuming that the proportion of resting cysts in the rDNA pool is *cyst%*, and their fraction in the rRNA pool is negligible (about 0.02% to 0.5% relative to a vegetative cell of *Colpoda* spp.), equation number 7 in Table 1 can be alternatively expressed as equation number 11 in Table 1, then *cyst%* can be assessed using a function of both  $rRNA_{\text{total}}/rDNA_{\text{total}}$  and cell size (Table 1, equation number 12).

According to reference 9, the per-cell rRNA CNs in the log-phase cells of *E. vannus* and *S. sulcatum* were at similar levels as the ones in *Colpoda* cells of similar cell sizes [the  $\lg(\text{CV})$  ranging from 3.3 to 4.1] (Fig. 4B). However, these two marine species had ~30 to ~80 times more rDNA copies (~109,000 to ~263,000 per cell) than *C. steinii* cells (~1,300 to ~9,540 copies per cell) within the same cell size range (Fig. 4B). In other words, the previous data on *E. vannus* and *S. sulcatum* largely followed the scaling relationship between rRNA and CV of nonresting *Colpoda* ( $R^2 = 0.86$ ;  $P < 0.001$ ) described herein but was not consistent with the rDNA-CV relationship described in the present study ( $R^2 = 0.05$ ;  $P < 0.001$ ).

Interestingly, based on a combination of data sets comprising those previously reported for *Euplotes vannus* and *Strombidium sulcatum* ( $n = 8$ ) (9) along with the present data for *Colpoda* spp. ( $n = 4$ ), the maximum growth rate ( $r$ ) of these species at a given culturing temperature ( $t$ ) can be well predicted by  $rDNA_{\text{CNPC}}$  ( $R^2 = 0.89$ ;  $P < 0.001$ ;  $n = 11$ ) (Table 1, equation number 13; Fig. 4C) and ratio of  $rRNA_{\text{CNPC}}/rDNA_{\text{CNPC}}$  ( $R^2 = 0.76$ ;  $P < 0.001$ ;  $n = 12$ )

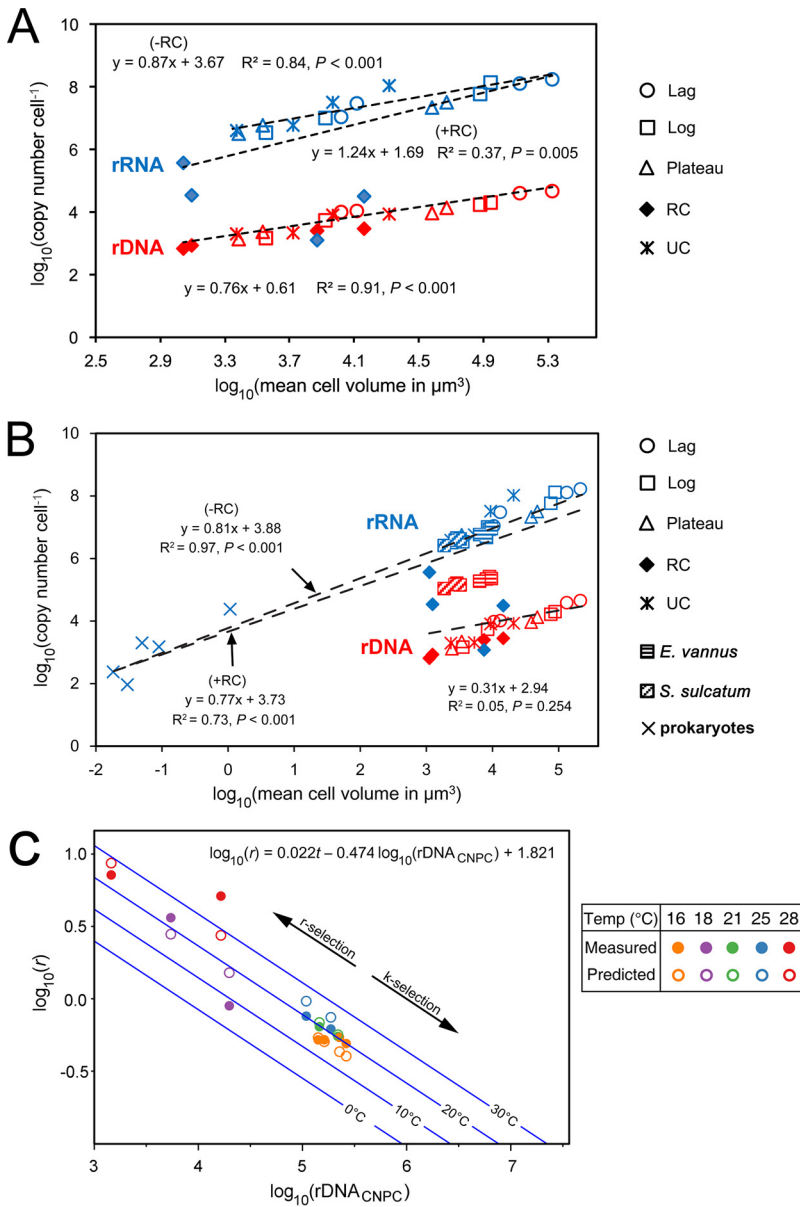


**FIG 4** Scaling relationships among ribotypic traits, growth rate, and cellular attributes. (A) The per-cell rDNA and rRNA copy numbers (CNs) in two *Colpoda* species across life cycle stages were significantly related to cell volume. (B) Scaling relationships based on a combined data set consisting of two *Colpoda* species (present study), *Euplotes vannus*, and *Strombidium sulcatum* and five prokaryotic species (9). The per-cell rRNA CNs are better predicted using cell volume when resting cysts (indicated by four symbols of solid diamond in blue) are excluded from the regression analysis (-RC) than when the resting cystic data are incorporated (+RC). The rDNA CNs of *E. vannus* and *S. sulcatum* were much higher than those of *Colpoda* cells with similar size ranges, suggesting that rDNA CN and CV relationship may be conserved among closely related taxa but becomes inconsistent among distant taxa. (C) Maximum growth rates ( $r$ ) of *Colpoda steinii*, *C. inflata*, *E. vannus*, and *S. sulcatum* can be well predicted by rDNA CN per cell (CNPC) and temperature ( $t$ ). Lines in blue denote predicted growth rate-CNPC relationships at 0, 10, 20, and 30°C. The amount of rDNA copies in genomes is inversely related to the growth potential of the cell, which might underline  $r$  and  $K$  selection of these organisms. RC, resting cysts; UC, unstable cysts.

(Table 1, equation number 14) but poorly by  $\text{rRNA}_{\text{CNPC}}$  ( $R^2 = 0.34; P = 0.064; n = 12$ ) (Table 1, equation number 15) or CV ( $R^2 = 0.33; P = 0.069; n = 12$ ) (Table 1, equation number 16).

**Single-cell landscape of rDNA and rRNA variants.** Processing the high-throughput sequencing data of 18S rDNA and cDNA (rRNA) amplicons of individual clones indicates that application of the DADA2 pipeline effectively filtered out error amplicon

**TABLE 1** Fitting equations linking ribotypic traits with phenotypic traits in ciliated protists<sup>a</sup>

No.	Response variable	Explanatory variable	Fitting equation	R <sup>2</sup>	P	n	Data source and assumption
1	log <sub>10</sub> (rDNA <sub>CNPC</sub> )	CV	0.76 log <sub>10</sub> (CV) + 0.61	0.91	<0.001	20	<i>Colpoda</i> spp.
2	log <sub>10</sub> (rDNA <sub>CNPC</sub> )	ESD	2.28 log <sub>10</sub> (ESD) + 0.396	0.91	<0.001	20	As above
3	log <sub>10</sub> (rDNA <sub>total</sub> )	N, ESD	log <sub>10</sub> N + 2.28 log <sub>10</sub> (ESD) + 0.396	0.91	<0.001	20	As above
4	log <sub>10</sub> (rRNA <sub>CNPC</sub> )	CV	1.24 log <sub>10</sub> (CV) + 1.69	0.37	0.005	20	<i>Colpoda</i> spp.; resting cysts are considered
5	log <sub>10</sub> (rRNA <sub>CNPC</sub> )	CV	0.87 log <sub>10</sub> (CV) + 3.67	0.84	<0.001	16	<i>Colpoda</i> spp.; resting cysts are not considered
6	log <sub>10</sub> (rRNA <sub>total</sub> )	N, ESD	log <sub>10</sub> N + 2.61 log <sub>10</sub> (ESD) + 3.43	0.84	<0.001	16	As above
7	log <sub>10</sub> (rRNA <sub>total</sub> /rDNA <sub>total</sub> )	ESD	0.33 log <sub>10</sub> (ESD) + 3.034				Derived from equation no. 2 and 6
8	log <sub>10</sub> (rDNA <sub>CNPC</sub> )	MV	0.90 log <sub>10</sub> (MV) + 1.44	0.93	< 0.001	16	<i>Colpoda</i> spp.; data not available for unstable cysts
9	log <sub>10</sub> (rRNA <sub>CNPC</sub> )	MV	1.70 log <sub>10</sub> (MV) + 2.28	0.50	0.002	16	As above
10	log <sub>10</sub> (rRNA <sub>CNPC</sub> )	MV	1.05 log <sub>10</sub> (MV) + 4.47	0.83	< 0.001	12	<i>Colpoda</i> spp.; resting cysts are not considered
11	log <sub>10</sub> (1 - rDNA <sub>rc</sub> /rDNA <sub>total</sub> )	ESD	log <sub>10</sub> (rRNA <sub>total</sub> /rDNA <sub>total</sub> - rRNA <sub>rc</sub> /rDNA <sub>total</sub> ) - 0.33 log <sub>10</sub> (ESD) + 3.034				Derived from equation no. 7
12	cyst%	rRNA <sub>total</sub> /rDNA <sub>total</sub> , ESD	1 - (rRNA <sub>total</sub> /rDNA <sub>total</sub> )/ (1,081 · ESD <sup>0.33</sup> )				Based on equation no. 11, assuming the rRNA pool in resting cysts (rRNA <sub>rc</sub> ) is negligible relative to the rDNA pool
13	log <sub>10</sub> (r)	rDNA <sub>CNPC</sub> , t	0.022t - 0.474 log <sub>10</sub> (rDNA <sub>CNPC</sub> ) + 1.821	0.89	<0.001	12	<i>Colpoda</i> spp., <i>Euplotes vannus</i> , and <i>Strombidium sulcatum</i>
14	log <sub>10</sub> (r)	rRNA <sub>CNPC</sub> /rDNA <sub>CNPC</sub> , t	0.036t + 0.289 log <sub>10</sub> (rRNA <sub>CNPC</sub> /rDNA <sub>CNPC</sub> ) - 1.355	0.76	<0.001	12	As above
15	log <sub>10</sub> (r)	rRNA <sub>CNPC</sub> , t	0.057t + 0.229 log <sub>10</sub> (rRNA <sub>CNPC</sub> ) - 2.746	0.34	0.064	12	As above
16	log <sub>10</sub> (r)	CV, t	0.055t + 0.206 log <sub>10</sub> (CV) - 1.92	0.33	0.069	12	As above

<sup>a</sup>CV, cell biovolume; cyst%, the proportion of resting cysts in the rDNA pool, assuming that cystic fraction in the rRNA pool is negligible (about 0.02% to 0.5% relative to a vegetative cell of *Colpoda* spp.); ESD, equivalent spherical diameter; r, growth rate; rDNA<sub>CNPC</sub> and rRNA<sub>CNPC</sub>, rDNA and rRNA copy numbers per cell; rDNA<sub>total</sub> or N · rDNA<sub>CNPC</sub>, total rDNA copy number of a population that can be experimentally determined (for example, by using qPCR); rRNA<sub>total</sub> or N · rRNA<sub>CNPC</sub>, total rRNA copy number of a population; rRNA<sub>rc</sub> and rDNA<sub>rc</sub>, the total cellular rRNA and rDNA copy numbers in the resting cysts existing in a population; n, number of samples; N, the cell abundance of an idealized population of identical cell size; t, temperature.

sequence variants (ASVs). Consequently, a single ASV was obtained for *E. vannus* and *S. sulcatum* and 12 ASVs for each of the two *Colpoda* species (see Table S2 in the supplemental material). For the latter two species, ASV clones with sequence divergence lower than 1% were lumped into a single operational taxonomic unit (OTU) at a similarity cutoff of 99% (OTU<sub>99%</sub>) to offset the sequencing errors in order to examine the biological variations by counting OTU numbers (Table S2). In the following sections, for *E. vannus* and *S. sulcatum*, once multiple ASVs (equivalent to OTUs clustered at a 100% similarity level, i.e., OTU<sub>100%</sub>) and multiple OTU<sub>99%</sub> were detected, they were considered to reflect real biological polymorphisms of rDNA and rRNA.

A total of 123 rDNA and cDNA samples derived from 123 single cells of the four ciliate species were successfully sequenced. For all DADA2-filtered sequences of a single cell, one to multiple OTU<sub>99%</sub> were often detected in rDNA and rRNA pools as follows: in *C. steinii*, 1 to 5 OTUs, and in *C. inflata*, 1 to 4 OTUs. For OTU<sub>100%</sub>, in *E. vannus* 1 to 6 OTUs were detected and in *S. sulcatum* 2 to 6 OTUs (see Table S1 in the supplemental material). In each species, there was a single, numerically dominant OTU, the relative abundance of which varied widely (87% to 100%), depending on species, rDNA, or rRNA pools, life cycle stage, and temperature (Fig. 5A to D). Significant changes in the proportion of dominant OTUs were detected in rRNA pools but not in rDNA (Fig. 5A to D). Furthermore, the dominant rRNA-based OTU<sub>99%</sub> was present in significantly lower

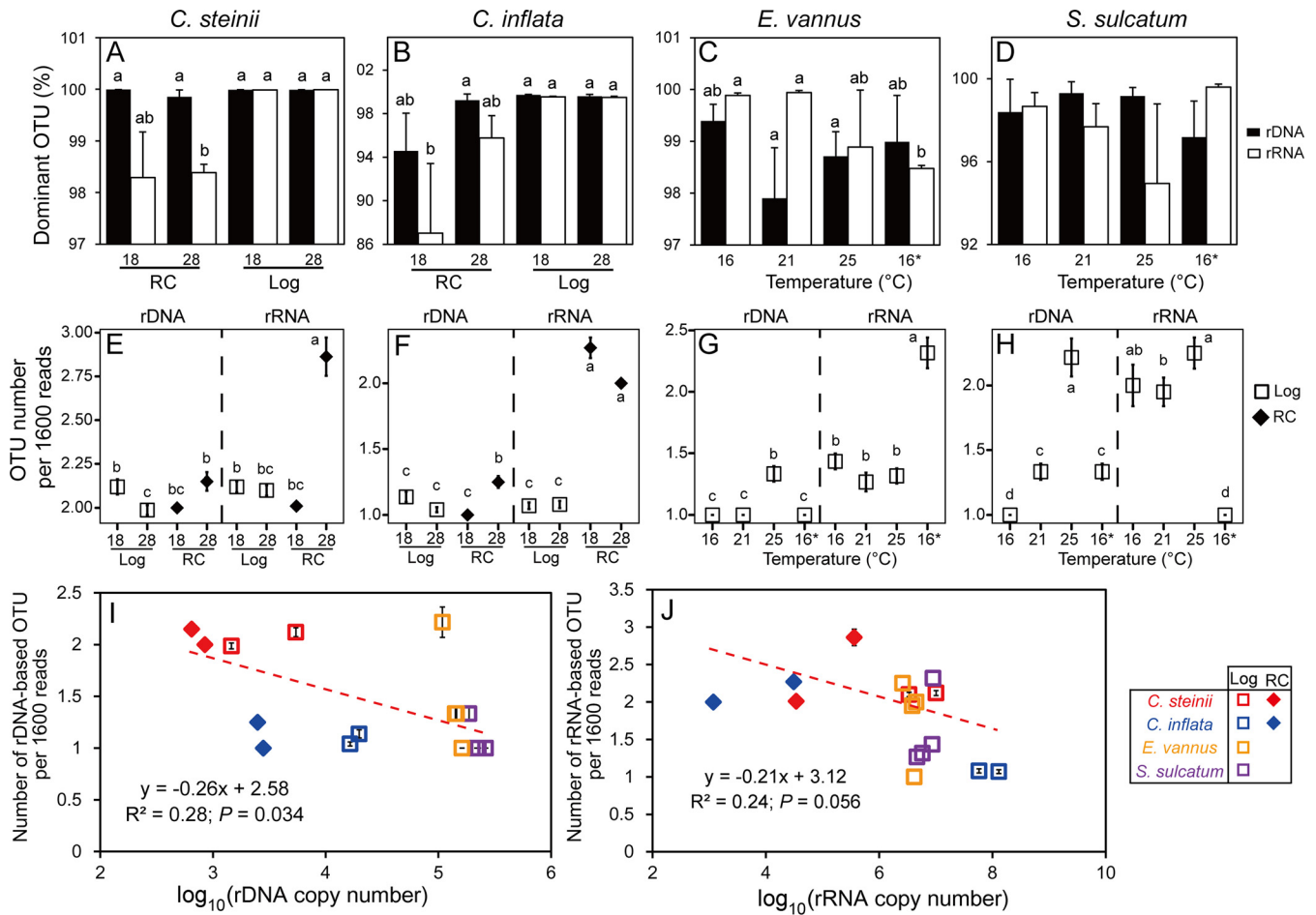


**FIG 5** Characterization of operational taxonomic units (OTUs) in rDNA and rRNA pools in single cells of four ciliate species. (A to H) Comparisons of the relative abundance of the most dominant OTU (A to D) and OTU numbers per 1,600 reads (E to H) between resting cysts (RC) and log-phase vegetative cells (Log) of *Colpoda steinii* and *C. inflata* at 18°C and 28°C and in a single log-phase cell of *Euplotes vannus* and *Strombidium sulcatum* at four temperatures. (I, J) Both rDNA (I) and rRNA-based OTU numbers (J) are negatively related to sequence number within a single cell. Two treatments not sharing common letters indicate significant differences (multiple pairwise comparisons,  $P < 0.05$ ). Note that the OTUs are defined at a sequence similarity cutoff of 99% for *C. steinii* and *C. inflata* and at 100% for *E. vannus* and *S. sulcatum* based on the results of sequencing and analysis of individual clones with 18S rDNA or cDNA fragments.

proportions in the resting cysts of *C. steinii* (at 28°C) and *C. inflata* (at 18°C) than in log-phase *Colpoda* cells at the same temperatures (Fig. 5A and B). Temperature generally did not affect the proportion of dominant OTU in any species (ANOVA,  $P > 0.05$ ) (Fig. 5A to D), except for two pairwise comparisons in the case of *E. vannus*, in which the dominant OTU<sub>100%</sub> of rRNA was present in a significantly lower proportion in the touchdown treatment ( $98.47 \pm 0.06\%$ ) than in the treatments at 16°C and 21°C (Fig. 5C).

The numbers of rDNA- and rRNA-based OTUs per 1,600 reads in single cells varied according to life cycle stage and temperature (Fig. 5E to H). At 28°C, resting cysts consistently had higher numbers of OTU<sub>99%</sub> than log-phase cells in both *Colpoda* species ( $P < 0.05$ ) (Fig. 5E and F). The log- versus resting-phase cells of *C. steinii* at higher temperature had fewer rDNA-OTU<sub>99%</sub>, while the resting- versus log-phase cells of *C. inflata* had more ( $P < 0.05$ ) (Fig. 5E and F). For *E. vannus* and *S. sulcatum*, the highest numbers of rDNA-based OTU<sub>100%</sub> were consistently detected at 25°C ( $P < 0.05$ ) (Fig. 5G and H). Nevertheless, the number of rRNA-based OTU<sub>100%</sub> peaked at 25°C in *S. sulcatum* and at 16°C in *E. vannus* ( $P < 0.05$ ) (Fig. 5G and H). Regression analysis based on single-cell data of all four species indicated that the number of OTUs in the rDNA pool was significantly and negatively related to cellular rDNA CN ( $R^2 = 0.28; P = 0.034$ ) (Fig. 5I), while the number of OTUs in rRNA pool

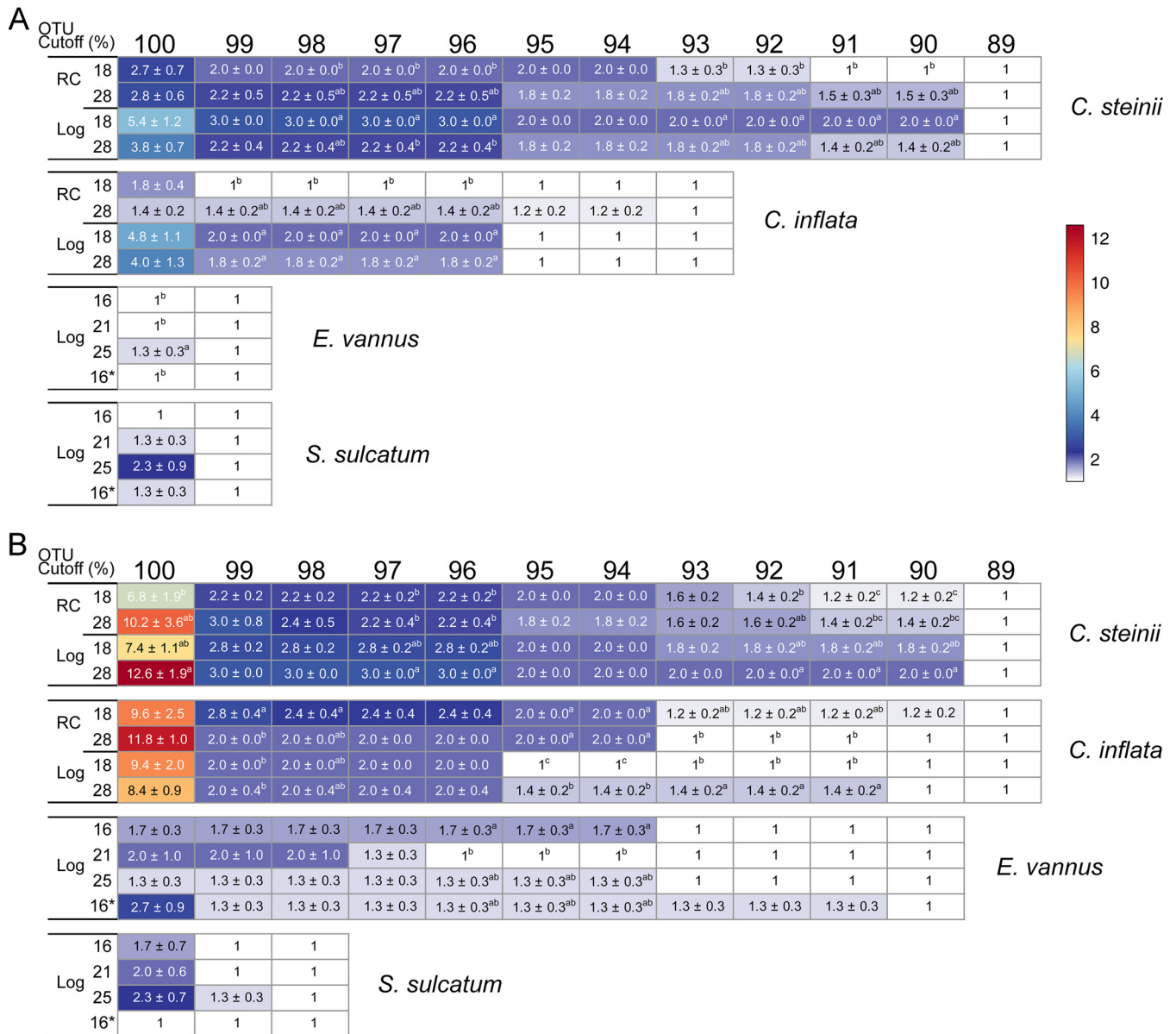


**FIG 6** Variation in the numbers of OTUs in rDNA (A) and rRNA (B) pools of single cells of ciliated protists. The OTUs were defined at a sequence similarity threshold ranging from 89% to 100%. The nominal maximum intraindividual rDNA and rRNA sequence differences of the four species ranged from 1% (in *S. sulcatum*) to 10% (in *C. steinii*). Two treatments not sharing common superscript letters indicate significant differences (multiple pairwise comparisons,  $P < 0.05$ ). The color bar indicate number of OTUs per cell. The asterisk indicates the touchdown treatment at 16°C.

was marginally and negatively related to cellular rRNA CN ( $R^2 = 0.24$ ;  $P = 0.056$ ) (Fig. 5J). However, analogous relationships between rDNA and rRNA OTU numbers and cell volume were not significant ( $P > 0.66$ ) (see Fig. S5 in the supplemental material).

**Divergence in rDNA and rRNA sequences in a single cell and its effect on OTU clustering.** By clustering all of the rDNA variants obtained from single-cell samples into OTUs at a series of gradually lower cutoffs of sequence similarity, the numbers of identified OTUs generally decreased (Fig. 6A). At the 97% cutoff, an average of 2.0 to 3.0 rDNA-based OTUs remained for *C. steinii* and 1.0 to 2.0 for *C. inflata*. The observed OTU numbers leveled off to 1 (or insignificantly different from 1) when the cutoff decreased to 89% in *C. steinii* and 95% in *C. inflata* (Fig. 6A). A single DNA-based OTU was identified for *E. vannus* and *S. sulcatum* at the 99% cutoff. Taking the sequencing errors that remained after DADA2 filtering into account (1% in the two *Colpoda* species and nil in *E. vannus* and *S. sulcatum*) (Table S2), it is estimated that the real maximum differences

among the rDNA variants in single cells of these species were 10%, 4%, 1%, and 1%, for *C. steinii*, *C. inflata*, *E. vannus* and *S. sulcatum*, respectively.

For all species, the sequence divergence of rRNA molecules was generally higher than that of rDNA (Fig. 6B). *Colpoda steinii*, *C. inflata*, and *E. vannus* had multiple (2.2 to 3.0, 2.0 to 2.4, and 1.3 to 1.7) OTUs at the 97% cutoff but only 1 OTU when the cutoff was raised to 89%, 90%, and 93%, respectively. Nevertheless, the number of rRNA OTUs in *S. sulcatum* was rapidly reduced at the 99% cutoff. The differences in rRNA sequences are estimated up to 10%, 9%, 7%, and 1% in *Colpoda steinii*, *C. inflata*, *E. vannus*, and *S. sulcatum*, respectively (Fig. 6B). At the 97% cutoff, significantly different rDNA-based OTU numbers were frequently identified between resting and log-phase cells of *Colpoda* spp. (Fig. 6A); however, this was never the case between any two temperature treatments in any species (Fig. 6A and B).

## DISCUSSION

**Ribotype copy number variations across different phases of growth and cystic forms.** Substantial variations in rDNA and/or rRNA quantities have been previously recorded in a range of protistan species at various phases of growth or physiological states (e.g., a *Tetrahymena* ciliate [33], a raphidophyte [34], a foraminifer strain [10], and dinoflagellates [35–37]). Nevertheless, this study provides the first evidence of linkage between ribotypic and phenotypic traits in ciliated protists. Specifically, the per-cell CN and cellular concentrations of rRNA and rDNA molecules, along with their CN ratio were quantitatively linked with cell and macronuclear sizes. This was a consistently observed relationship across all growing phases and dormant cystic forms.

Artificially induced unstable cysts constituted an exception to this observation. The per-cell rDNA and rRNA CNs as well as cell size (Fig. 2A and B and Fig. 3A and B) were significantly reduced in these cysts. Freezing raw environmental samples (e.g., soil, sediment, or water) temporarily to preserve microbiomes is occasionally used in molecular ecology. Herein, we show that this practice might artificially alter both phenotypic and ribotypic traits of cyst-forming protists, leading to underestimation of their biomass and proportions of rDNA and rRNA quantities in the ribotypic pools. Nevertheless, chilling treatment is a simple, nondestructive approach that arrests growing cells at the unstable cyst stage, thus narrowing down the cell size spectrum of a population consisting of different-sized cells in various growth phases, while preserving cell numbers in the original samples. Thus, chilling treatment has the potential to enhance the accuracy in estimating population abundances.

We provide evidence that both unstable and resting cysts of *Colpoda* follow the rDNA CN-CV relationship (Fig. 4A; Table 1, equation numbers 1 and 2), so their biomass can be reasonably predicted in rDNA-based molecular surveys. Nevertheless, compared to unstable cysts, resting cysts have disproportionately fewer rRNA molecules, which could be attributed to the former having a higher metabolic rate than the latter (38). Based on the ribotypic distinctness of resting cysts, we propose a theoretical framework to estimate their proportion in the rDNA pool of a population using experimentally determined rRNA/rDNA ratio of a given *Colpoda* species. The proposed framework supports the use of the rRNA/rDNA ratio as a predictor of protistan dormancy in environmental studies. Importantly, the framework emphasizes taking cell size into account (see equation number 12 in Table 1), which is especially relevant when comparing cellular activity across species or taxa of contrasting cell sizes. Thus, species- or taxon-specific qPCR assays could be applied in future studies for quantifying cysts of *Colpoda* and/or other protists in environmental samples.

**Cellular rRNA content scales consistently with cell size, but maximum growth rate depends on rDNA content.** Previously, a scaling relationship between rRNA content and cell size of log-phase cells of two protist species and five species of bacteria and archaea was proposed (9). Herein, we show that the scaling relationship holds across life cycle stages, indicating that the scaling law between rRNA content and cell/body size applies not only to macro-organisms but microbes as well (39). Nevertheless, the scaling relationship did not apply to resting cysts, as their rRNA content was significantly lower than expected given their cell size. This indicates that rRNA quantity is a suitable molecular indicator for providing a biomass-based view of active members in communities. In support of

this, previous studies of mock protistan communities showed consistent patterns when using rRNA and cell counting approaches (40).

Unlike rRNA, the scaling relationship between rDNA and cell volume was not uniform for any of the four ciliate species examined. Instead, two separate functions were applied, one for *Euplotes* and *Strombidium* ( $rDNA \sim CV^{0.44}$ ) (9) and another for *Colpoda* spp. ( $rDNA \sim CV^{0.76}$ ) (this study). This is primarily due to the much higher cellular rDNA content in *E. vannus* and *S. sulcatum* (23 to 59 copies per  $\mu\text{m}^3$ ) than in the similarly sized cells of *Colpoda steinii* and *C. inflata* (0.2 to 0.8 copies per  $\mu\text{m}^3$ ) (Fig. 4B). The disproportion between per-cell rDNA copy number and cell size has been previously pointed out (41). The variable rDNA content of Spirotrichea and Colpodea may stem from their genomic distinctness. Spirotrichean ciliates are well known for their highly polyploidized genomic macronuclear DNA (26). Higher rDNA content also implies higher genomic DNA content and larger macronuclear volumes (42). In support of this, both *E. vannus* and *S. sulcatum* have disproportionately large macronuclei (N/C ratios of about 4.71% and 2.73%, respectively) that do not correspond to the predicted values (1.57% and 2.43%) derived from the *Colpoda*-based model (Fig. 2E and F). This indicates that larger macronuclear size does contribute to higher rDNA content in these two spirotricheans. Even when their “enlarged” macronuclear sizes are taken into consideration, their calculated per-cell rDNA copy numbers according to the *Colpoda*-based function (equation number 8 in Table 1) are only about 1/2 and 1/16 of those experimentally determined. This suggests that the high rDNA content of spirotricheans is not just due to their unusual phenotype (enlarged macronuclei) but that certain, as yet undiscovered, mechanisms for genomic innovation may also be at play.

Interestingly, *C. steinii* grew 7 to 12 times faster than *E. vannus* and *S. sulcatum*, despite these three species having comparable cell size and cellular rRNA content. When predicting growth rate (Table 1, equation numbers 13 and 15), the model parameterized using rDNA performed much better than the one using rRNA. Thus, besides temperature (which modulates cell size via the temperature-size rule [43]), cellular rDNA content is an important factor in determining generation time of these ciliated protists. This observation suggests that growth rate is not only determined by rRNA content, as proposed in the growth rate hypothesis (44), but can also be modified by rDNA contents. In other words, growth rate depends mainly on rDNA, when the cells have similar cell sizes or rRNA contents (see Fig. 4B).

Existing studies on genomic content and growth rates of various organisms can shed light on our understanding of the mechanisms underlying modulation of cell growth rate and relationship with rDNA content. For instance, haploid cells of budding yeast grew more rapidly than their diploid counterparts of larger cell size. The observed fitness difference was attributed to their cell surface to volume ratio. Specifically, growth rate was dependent on the transfer of products into cytoplasm generated upon hydrolysis of organic phosphorous by a cell surface-bearing acid phosphatase (45, 46). The surface-to-volume-ratio theory does not seem to apply to phagotrophic ciliates, which graze on food particles through their cytostome and digest them inside cytoplasmic food vacuoles. Nevertheless, the lower nuclear to cell volume ratio of *C. steinii* may allow for a larger cytoplasmic space to accommodate additional food vacuoles, enabling digestion of more bacterial prey and maintenance of a higher rate of material supply for growth than *E. vannus* and *S. sulcatum*. Spirotricheans have a high content of rDNA and genomic DNA, both of which are particularly P and N rich. Thus, these ciliates need element-rich resources and invest a longer time for DNA replication, synthesis of associated proteins, and cell division (47). Conversely, the similarly sized colpodean ciliate *C. steinii* with fewer rDNA copies and a more streamlined genome would save more P and N to synthesize rRNA and assemble ribosomes for rapid growth.

**Richness and composition of rDNA and rRNA variants across life cycle stages and at different temperatures.** In the present study, the error rate of high-throughput sequencing was offset on the basis of individual clones of amplicons. Even so, low to high levels (1% to 10%) of sequence divergence were still identified in single cells, indicating high likelihood of the observed variants of 18S rDNA and rRNA of ciliated protists being of biological origin. The extent of divergence observed in this study is comparable to that previously

uncovered using high-throughput sequencing (13% in radiolarians [18] and up to about 16% in a *Protocruzia* ciliate [48]). Previous studies on rDNA polymorphisms using clone libraries and Sanger sequencing yielded lower intragenomic divergence (<2%) in ciliates (9, 21, 41) and diatom species (0.57% to 1.81% [49]), while divergence was moderate (about 5%) in foraminifera (17). It has been speculated that use of polymerases of varying fidelity in separate studies might affect polymorphism estimations (21). Herein, identical experiments (e.g., polymerase and PCR thermal cycling conditions) were performed and expected to yield similar error rates. This suggests that the observed distinct divergence rates among the four ciliates might be dependent on species identity. A possible reason for this could be that the species with low per-cell rDNA copy numbers tend to have more rDNA variants (Fig. 5I), providing a higher chance to explore cellular rDNA variant space and thus resulting in a higher sequence divergence (Fig. 6A).

The results confirm our expectation that multiple and less-abundant (relative abundance  $\leq 13\%$ ) rRNA variants (or OTU<sub>99%</sub> of *Colpoda* spp. and OTU<sub>100%</sub> of *E. vannus* and *S. sulcatum*) are transcriptionally expressed in single cells of the protists studied herein (Fig. 6B). These variants could combine with ribosomal proteins, giving rise to extremely high ribosomal heterogeneity in these ciliates. Such a high diversity of ribosomes in single-celled eukaryotes is surprising because these organelles have long been thought of as a homogeneous cellular machinery. A notable exception is the parasitic protist, *Plasmodium berghei*, in which two structurally distinct 18S rRNA transcripts were found (22). Recent studies have suggested that ribosomal variants could preferentially bind different mRNAs to regulate gene expression and corresponding phenotypes of bacteria under stress conditions (24, 25, 50). Given the high intracellular rDNA diversity in diverse protistan groups, the significance of ribosomal heterogeneity in the context of physiological and ecological adaptations of protists inhabiting various ecosystems would be an interesting topic to explore.

Pairwise comparisons also support relationships between rDNA- and rRNA-based OTU richness and life cycle stage and temperature (Fig. 5E to H), indicating the dynamic nature of ribotypic composition and its tight coupling with physiological status in ciliates. More specifically, the richness of rRNA-based OTU<sub>99%</sub> composition in the cysts was higher than that in log-phase cells. This could be attributed to shrinkage of the rRNA pool during encystment accompanied by loss of cellular rRNA copies of the dominant variant and maintenance of minor ones (Fig. 5A and B). Functionally, keeping more rRNA OTUs (and by extension, a higher diversity of ribosomes) in the resting cysts may be significant for soil ciliates in maintaining a high metabolic potential to readily respond to favorable environmental conditions. Resting cysts have specialized mRNA and proteins (51), and *C. inflata* is known to undergo demethylation of macronuclear DNA during encystment (52). Further investigations are needed to explore the mechanistic links between DNA methylation, rRNA-derived ribosomal heterogeneity, and mRNA translation toward a better understanding of protistan adaptations and their biological and ecological roles.

**Concluding remarks.** In summary, the present study is the first to provide evidence for quantitative relationships between rDNA and rRNA copy numbers and cell size of protists across life cycle stages, illustrate a methodological framework for estimating the quantity of resting cysts, and show compositional changes in sequence variants during formation of resting cysts and in response to temperature. Although the findings on phenotype-ribotype coupling were based on ciliate models in this study, variations in genome content across life cycle stages and under different conditions have been reported for other protists, e.g., *Giardia* (53) and amoeba species (54). This suggests that relationships among ribotype numbers, genomic content, cell and nuclear size, and growth rate likely exist in many groups of protists as previously predicted in references 42 and 55. Our findings have tentatively important implications for microbiome and microbial biogeographic studies of microbial eukaryotes. (i) We demonstrate substantial changes in cellular contents of rDNA and especially rRNA across life cycle stages of protists. This suggests that, even if the cell abundance of each species in a community remains unchanged, the relative abundances of these molecules among protistan species, and hence the inferred diversity and community structure,

can be highly variable depending on life cycle stage and physiological shifts. This layer of biological complexity should be considered in metabarcoding approaches focused on detecting protistan diversity alterations, ecological responses and adaptations to environmental changes, and biotic interactions (e.g., water and prey availability and warming), and thus has functional and ecological significance. (ii) Cellular rRNA quantity generally scaled much better with cell volume than genomic rDNA, which could be related to genome duplication and reduction, or alteration of ploidy levels among protistan taxa. This implies that rRNA is a better molecular marker than rDNA for mapping biomass partitioning in multispecies communities, especially among active members. (iii) In contrast, growth rate of protistan cells could be more accurately predicted using cellular rDNA content rather than rRNA, rRNA/rDNA copy number ratio, or cell size. Linking this ribotypic trait to cellular growth opens a window for a taxon-specific view of microbial production in various environments. (iv) Protistan diversity, community composition, rare-to-abundant transition, seasonality, biogeographical patterns, dynamic responses to perturbations, as well as ecological and biogeochemical functions in soil, planktonic, and benthic systems are all affected by dormancy of cysts (1, 5, 11, 12). Our work illustrates a potential resolution in determining the functional and ecological importance of protistan dormancy across time and space by simultaneously quantifying rDNA and rRNA molecules.

Our results of sequencing and downstream analyses of single-cell rDNA and rRNA variants have implications for ciliate/protistan diversity surveys using metabarcoding. (i) Despite using a sensitive pipeline (e.g., DADA2) for quality filtering, low levels of sequencing errors (<1%) could still exist in 18S rDNA and rRNA amplicon sequences of some species; therefore, it is generally recommended that a 99% sequence similarity threshold be applied if intragenomic polymorphism is of interest. (ii) Inferring species-level diversity using a sequence similarity of 97% can lump intragenomic sequence polymorphisms in some, but not all, species. In addressing the changing patterns of protistan richness, this part of richness inflation can be relieved if the inflated species are present in all or most samples or they account for substantially low sequence proportions. Otherwise, the intragenomic polymorphisms of rDNA and rRNA sequences remain an issue that potentially undermines our capability in estimating and predicting protistan richness in natural or complex communities.

## MATERIALS AND METHODS

**Source organisms, cultivation, and treatments.** Two cyst-forming, soil ciliate species, *Colpoda steinii* and *C. inflata*, were collected from a coastal apple orchard in Yantai, Shandong, China. The protists were cultivated and isolated using the nonflooded Petri dish method (56). *Euplotes vannus* and *Strombidium sulcatum* were originally isolated from the coastal waters off Qingdao (Shandong, China) and have been maintained in the laboratory since then. Cultivation of these ciliates and monitoring of their growth rate were as previously described (9). The *Colpoda* species were incubated for 10 days at 18°C and 28°C and underwent distinct phases (lag, log, and plateau) during that time. Population growth at temperatures lower than 18°C or higher than 28°C was strongly inhibited and thus not investigated further. Following the plateau phase, both species consistently formed resting cysts, probably due to overpopulation and food depletion. Phase-specific cells (including the resting cysts) were individually isolated to determine both phenotypic and ribotypic traits at the single-cell level. Two marine species, *E. vannus* and *S. sulcatum*, were reared at 16°C, 21°C, and 25°C. For these two taxa, only cells in log phase were investigated. In order to explore possible footprint effect of the higher temperature on ribotypic traits, an additional “touchdown” treatment (designated with an asterisk) was set as previously described (9). Briefly, a few individuals of the treatments maintained at 25°C for 30 d were transferred and recultured at 16°C for a month. All treatments were done in triplicate.

Many ciliate species form unstable cysts when temperature shifts beyond certain limitations in a short time period (30). These are generally larger than resting cysts, undergo complete ciliary dedifferentiation, and return to vegetative cell state in a few hours. We tried obtaining unstable cysts of *Colpoda* by chilling cells for various periods of time. Tubes containing actively growing vegetative cells were transferred in three separate conditions as follows: ice-water mixture (0°C) and chemostat reactors set at 4°C and 10°C. Twenty microliters of culture solution were used to identify and count vegetative cells and unstable cysts using a stereomicroscope (XLT-400; Guiguang, China) at ×45 magnification. Cultures were monitored every 0.5 to 2 h to determine the optimal time period for achieving the highest yield of unstable cysts. All chilling treatments were performed in triplicate. Since unstable cysts have high phenotypic plasticity, relevant phenotypic and ribotypic traits of this temporary stage were also determined and analyzed.

**Determination of growth rate, cell volume, and macronuclear size.** Cell abundances were determined once a day (Fig. 1A). Estimation of cell volume (CV) and calculations of growth rates of the two *Colpoda* species during the log phase were as previously described (9). At least 18 cells from each growth stage were randomly selected and fixed with Lugol's solution (final concentration, 2%). Fixed

vegetative cells and resting and unstable cysts of both *Colpoda* species were ellipsoid; thus, their cell volume was calculated according to the standard formula for a spheroid. Cell and macronuclear sizes of the *Colpoda* species were also determined based on specimens fixed with Bouin's solution and stained using protargol impregnation (57). This approach reveals many morphological features of ciliates in detail, which enabled examination of the relationship between cell and macronuclear size.

**Cell lysis, DNA extraction, and cDNA synthesis.** Cell lysis, DNA extraction, and RNA transcription of single cells followed previous works (9). In brief, ciliate cells/cysts were washed and transferred into nuclease-free PCR tubes for cell lysis. Eighteen tubes (replicates), each containing a single intact cell, were set up for cell lysis and nucleic acid extraction. Each cell was suspended in 1  $\mu$ l of distilled water followed by addition of 2  $\mu$ l of mixed solution containing 1.9  $\mu$ l 0.2% Triton X-100 (Solarbio, Beijing, China) and 0.1  $\mu$ l of recombinant RNase inhibitor (TaKaRa Biomedicals, Japan). The tubes were gently flicked, briefly centrifuged, and incubated at room temperature for 10 min. Nuclease-free PCR tubes, microtubes, and micropipette tips (Axygen Scientific, CA, USA) were used for all manipulations. One microliter of the cell suspension was used to extract genomic DNA, while 2  $\mu$ l was used for RNA reverse transcription. Genomic DNA extraction was performed with a REExtract-N-Amp tissue PCR kit (Sigma, St. Louis, MO) according to the manufacturer's instructions, except the suggested volume of each reagent was modified to 1/50 as previously described (58).

The RNA reverse transcription of single cells was as previously described (9). The remaining 2  $\mu$ l of cell suspension was mixed with 1  $\mu$ l random hexamers B0043 (10  $\mu$ M; Sangon, China) and 1  $\mu$ l of deoxy-nucleoside triphosphate (dNTP) mix (10  $\mu$ M). Tubes were incubated at 72°C for 3 min and then transferred immediately onto ice. SuperScript III reverse transcriptase kit (Invitrogen, CA, USA) was used for reverse transcription of RNA. The total volume used for PCR was 12.42  $\mu$ l, which was made up of 4  $\mu$ l rRNA template, 3  $\mu$ l 5 $\times$  first strand buffer, 0.3  $\mu$ l SuperScript III reverse transcriptase, 1  $\mu$ l 0.1 M dithiothreitol (DTT), 2  $\mu$ l Betaine (Sigma-Aldrich), 0.12  $\mu$ l 0.5 M MgCl<sub>2</sub>, 1  $\mu$ l RNase inhibitor (Roche, Germany), and 1  $\mu$ l diethyl pyrocarbonate (DEPC)-treated water. The following program was run on a thermal cycler (Biometra, Göttingen, Germany) with an initial temperature of 50°C for 90 min followed by 10 cycles at 55°C for 2 min and a final step at 70°C for 15 min. Both the DNA and synthesized cDNA were stored at -80°C for subsequent assays.

**Quantitative real-time PCR.** To quantify 18S rDNA and rRNA (cDNA) copy numbers in *Colpoda* cells, the newly designed species-specific primers CsQ207f (5'-TAACCTGGCAACAGGA-3') and CsQ459r (5'-TGCAATCTGCAACCCCA-3') were used in qPCR assays to amplify a 252-bp fragment of the 18S rRNA gene of *C. steinii*. The eukaryote-specific primers EUK345f (5'-AAGGAAGGCAGCAGCG-3') and EUK499r (5'-CACCAGACTTGCCCTCYAAT-3') (59) were used to amplify a 149-bp fragment of *C. inflata*. Two standard curves were constructed with the sequences of the two *Colpoda* species as previously described (19). All of the qPCRs were performed on a 7500 Fast real-time PCR system (Applied Biosystems) with the following program: 95°C for 7 min followed by 45 cycles of 95°C for 30 s, 55°C (60°C for *C. inflata*) for 1 min, and 72°C for 1 min (77°C for 25 s for *C. inflata*). The data were collected at 72°C and 77°C for *C. steinii* and *C. inflata*, respectively; all reactions ended with a melt curve stage from 60°C to 95°C (gradually increasing by 0.3°C). Standard curves were generated using log<sub>10</sub> number of copies versus the threshold cycle (C<sub>T</sub>). The goodness of fit (R<sup>2</sup>) ranged from 0.998 to 1.000, with the amplification efficiency ranging from 98% to 108.9% (see Fig. S1 in the supplemental material). All qPCRs were performed in triplicate. Controls without templates resulted in undetectable values for all samples. As the samples of rRNA also contained genomic rDNA, the rRNA (cDNA) copy numbers were calculated by subtracting the rDNA CNs from the sum of rDNA and cDNA copy numbers.

**Single-cell high-throughput sequencing.** The obtained genomic DNA and synthesized cDNA from single cells of each of the four ciliate species was used for high-throughput sequencing. These included cells of *Colpoda steinii* and *C. inflata* at two typical stages (i.e., vegetative cells in log phase and resting cysts) and grown at two temperatures (18°C and 28°C), plus *Euplotes vannus* and *Strombidium sulcatum* at log phase grown at four temperature treatments (i.e., 16°C, 21°C, 25°C, and 16°C\* [9]). The genomic DNA of cDNA samples was completely digested at 37°C using a TURBO DNA-free reagent kit (Invitrogen), in which the digestion mixture consisted of 1  $\mu$ l cell lysate, 1  $\mu$ l 10 $\times$  TURBO DNase buffer, 1  $\mu$ l TURBO DNase (2 units  $\mu$ l<sup>-1</sup>), and 7  $\mu$ l nuclease-free water. The optimal DNase dose (2 units) and incubation time (1 h) for DNA degradation were achieved by trail tests, and complete degradation was verified by PCR amplification of 35 cycles and absence of target bands on 1.5% agarose electrophoresis gel (see Fig. S2 in the supplemental material).

The V4 hypervariable region of 18S rDNA and cDNA in *C. steinii* and *C. inflata* (373 and 374 bp in length, respectively) was amplified using the eukaryotic-specific primers TAReuk454FWD1 (5'-CCAGCASCYGGTAATCC-3') and TAReukREV3 (5'-ACTTTCGTCTTGATYRA-3') (60). The V1 to V3 regions of 18S rDNA and cDNA in *E. vannus* and *S. sulcatum* (445 and 446 bp in length) were amplified with primers Euk82F (5'-GAADCTGYGAAYGGCTC-3') and Euk516R (5'-ACCAGACTTGCCCTCC-3') (61, 62). A 6-bp sample identifying barcode was added to both primer sequences. The PCR solution (30  $\mu$ l) contained 10 ng of DNA or cDNA, 0.2  $\mu$ M each primer, and 15  $\mu$ l of 2 $\times$  Phusion high-fidelity PCR master mix (New England BioLabs). All PCR amplification reactions were carried out on a T100 thermal cycler (Bio-Rad) as follows: initial pre-denaturation at 98°C for 1 min followed by 30 cycles of denaturation at 98°C for 10 s, annealing at 50°C (56°C for the two marine ciliates) for 30 s, and elongation at 72°C for 30 s, with a final extension step at 72°C for 5 min. The libraries were prepared using a NEBNext Ultra DNA library prep kit. Paired-end 250-bp and 300-bp sequencing were executed on HiSeq and MiSeq platforms (Illumina, USA) for the soil and marine species, respectively. A total of 80 single-cell rDNA and rRNA pools of the two *Colpoda* species were sequenced. For each *Colpoda*, 20 cells were used to sequence DNA and another 20 for cDNA. There were five biological replicates for each treatment. Four samples failed to be amplified, resulting in 39 samples of cells at log phase and 37 samples of resting cysts. A

total of 48 single cells of *E. vannus* and *S. sulcatum* were also sequenced. For each species, 24 cells were used to sequence DNA and 24 for RNA pools. Each treatment was run in triplicate.

To assess possible experimental errors during PCR amplification and high-throughput sequencing, four clone libraries of the 18S rDNA and cDNA (rRNA) amplicons for the four species were constructed as previously described (19). Five transformed clones were randomly and individually selected from each library and sequenced using MiSeq, as described above. Our expectations were the following: (i) the resulting reads of each species would be identical (any observed variants would represent sequencing errors), and (ii) only a single unique sequence would be retained for each species after sequencing errors were filtered out.

**Sequence data processing and analysis.** The rDNA and cDNA pools of the four ciliate species yielded a total of 8,478,407 reads (see Table S1 in the supplemental material). The primers were removed from the raw reads using Cutadapt v1.18 (63). The DADA2 and DECIPHER package v1.14.1 (64) were applied to model and correct substitution errors and filter and cluster the amplicons in R (v3.6.3 [65]). Reads were trimmed and filtered using the command “filterAndTrim” with the following parameters: minLen = 180, maxEE = c(2), maxN = 0, truncQ = 2, rm.phix = TRUE, multithread = TRUE. The filtered sequences were dereplicated using the function “derepFastq” to generate unique sequences. The error models were trained using the function “learnErrors” and used for sample inference of the dereplicated reads using the core function “dada” with pool argument set to pseudo to generate amplicon sequence variants (ASVs). Afterwards, forward and reverse reads were merged using the command “mergePairs,” and “removeBimeraDenovo” was used to check for chimeras. The “ldTaxa” command of package DECIPHER v2.14.0 (66) was used for taxonomic assignment using the SILVA\_SSU\_v138 training set as the reference database, and the reads assigned to each species were extracted using the tool *seqtk* (<https://github.com/lh3/seqtk>). The “deunique.seqs” command in Mothur was used to create a redundant fasta file from the ASVs fasta and sequence count file. For the treatments of each species, the redundant ASVs were further clustered into operational taxonomic units (OTUs) at a series of similarity thresholds ranging from 89% to 100% using UCLUST.

**Statistical analysis.** One-way ANOVA with least significant difference (LSD) *post hoc* test was performed to examine the significance ( $\alpha = 0.05$ ) of the growth phase-wise differences in phenotypic (i.e., cell volume, macronuclear volume, cell to macronuclear volume ratio) and ribotypic traits (per-cell rDNA and rRNA CNs and concentrations, rDNA/rRNA CN ratio). The maximum growth rates of two *Colpoda* species at two different temperatures were statistically compared using *t* test. Pearson correlation and linear regression analyses were carried out to explore associations between phenotypic and ribotypic traits or between ribotypic traits. All analyses were executed using the statistical software SPSS v.13.0 (SPSS, Chicago, IL).

**Data availability.** The reads from the high-throughput sequencing of eukaryotic 18S rRNA genes and transcripts are available under accession numbers [SRR10589967](https://ncbi.nlm.nih.gov/submit/seqs/SRR10589967) to [SRR10590042](https://ncbi.nlm.nih.gov/submit/seqs/SRR10590042) (*Colpoda steinii* and *Colpoda inflata*) and [SRR10590394](https://ncbi.nlm.nih.gov/submit/seqs/SRR10590394) to [SRR10590441](https://ncbi.nlm.nih.gov/submit/seqs/SRR10590441) (*Euplotes vannus* and *Strombidium sulcatum*). The reads obtained from individual clone sequencing are available under the BioProject accession number [PRJNA737167](https://ncbi.nlm.nih.gov/bioproject/PRJNA737167), with accession numbers [SRR14800224](https://ncbi.nlm.nih.gov/submit/seqs/SRR14800224) to [SRR14800243](https://ncbi.nlm.nih.gov/submit/seqs/SRR14800243).

## SUPPLEMENTAL MATERIAL

Supplemental material is available online only.

**SUPPLEMENTAL FILE 1**, PDF file, 0.7 MB.

## ACKNOWLEDGMENTS

This work was supported by grants from the Marine S & T Fund of Shandong Province for Pilot National Laboratory for Marine Science and Technology (Qingdao) (no. 2018SDKJ0406-4), the Innovation Group Project of Southern Marine Science and Engineering Guangdong Laboratory (Zhuhai) (no. 311021004), the Natural Science Foundation of China (no. 31572255, 41976128, and 31672251), the Research Fund Program of Guangdong Provincial Key Laboratory of Marine Resources and Coastal Engineering, and the Key Research Program of Frontier Sciences (QYZDB-SSW-DQC013).

We declare no conflicts of interest.

## REFERENCES

1. Corliss JO. 2001. Protozoan cysts and spores. John Wiley & Sons, Hoboken, NJ.
2. Padilla DK, Savello MM. 2013. A systematic review of phenotypic plasticity in marine invertebrate and plant systems. *Adv Mar Biol* 65:67–94. <https://doi.org/10.1016/B978-0-12-410498-3.00002-1>.
3. Mulot M, Marcisz K, Grandgirard L, Lara E, Kosakyan A, Robroek BJM, Lamentowicz M, Payne RJ, Mitchell EAD. 2017. Genetic determinism vs. phenotypic plasticity in protist morphology. *J Eukaryot Microbiol* 64:729–739. <https://doi.org/10.1111/jeu.12406>.
4. McQuoid MR, Hobson LA. 1996. Diatom resting stages. *J Phycol* 32:889–902. <https://doi.org/10.1111/j.0022-3646.1996.00889.x>.
5. Persson A. 2001. Proliferation of cryptic protists and germination of resting stages from untreated sediment samples with emphasis on dinoflagellates. *Ophelia* 55:151–166. <https://doi.org/10.1080/00785326.2001.10409482>.
6. Ross BJ, Hallock P. 2016. Dormancy in the foraminifera: a review. *J Foraminiferal Res* 46:358–368. <https://doi.org/10.2113/gsjfr.46.4.358>.
7. Caron DA, Countway PD, Jones AC, Kim DY, Schnetzer A. 2012. Marine protistan diversity. *Annu Rev Mar Sci* 4:467–493. <https://doi.org/10.1146/annurev-marine-120709-142802>.
8. Weider LJ, Elser JJ, Crease TJ, Mateos M, Cotner JB, Markow TA. 2005. The functional significance of ribosomal (r)DNA variation: impacts on the

- evolutionary ecology of organisms. *Annu Rev Ecol Evol Syst* 36:219–242. <https://doi.org/10.1146/annurev.ecolsys.36.102003.152620>.
9. Fu R, Gong J. 2017. Single cell analysis linking ribosomal (r)DNA and rRNA copy numbers to cell size and growth rate provides insights into molecular protistan ecology. *J Eukaryot Microbiol* 64:885–896. <https://doi.org/10.1111/jeu.12425>.
  10. Parfrey LW, Grant J, Katz LA. 2012. Ribosomal DNA is differentially amplified across life-cycle stages in the foraminifer *Allogromia laticollaris* strain CSH. *J Foraminif Res* 42:151–155. <https://doi.org/10.2113/gsfjr.42.2.151>.
  11. Fistarol GO, Legrand C, Rengefors K, Granéli E. 2004. Temporary cyst formation in phytoplankton: a response to allelopathic competitors? *Environ Microbiol* 6:791–798. <https://doi.org/10.1111/j.1462-2920.2004.00609.x>.
  12. Anderson DM, Rengefors K. 2006. Community assembly and seasonal succession of marine dinoflagellates in a temperate estuary: the importance of life cycle events. *Limnol Oceanogr* 51:860–873. <https://doi.org/10.4319/lo.2006.51.2.0860>.
  13. Erdner DL, Percy L, Keafer B, Lewis J, Anderson DM. 2010. A quantitative real-time PCR assay for the identification and enumeration of *Alexandrium* cysts in marine sediments. *Deep Sea Res Part 2 Top Stud Oceanogr* 57:279–287. <https://doi.org/10.1016/j.dsr2.2009.09.006>.
  14. Rivière D, Szczebara FM, Berjeaud J-M, Frère J, Hécharid Y. 2006. Development of a real-time PCR assay for quantification of *Acanthamoeba* trophozoites and cysts. *J Microbiol Methods* 64:78–83. <https://doi.org/10.1016/j.mimet.2005.04.008>.
  15. Blazewicz SJ, Barnard RL, Daly RA, Firestone MK. 2013. Evaluating rRNA as an indicator of microbial activity in environmental communities: limitations and uses. *ISME J* 7:2061–2068. <https://doi.org/10.1038/ismej.2013.102>.
  16. Pillet L, Fontaine D, Pawlowski J. 2012. Intra-genomic ribosomal RNA polymorphism and morphological variation in *Elphidium macellum* suggests inter-specific hybridization in foraminifera. *PLoS One* 7:e32373. <https://doi.org/10.1371/journal.pone.0032373>.
  17. Weber AA-T, Pawlowski J. 2014. Wide occurrence of SSU rDNA intragenomic polymorphism in foraminifera and its implications for molecular species identification. *Protist* 165:645–661. <https://doi.org/10.1016/j.protis.2014.07.006>.
  18. Decelle J, Romac S, Sasaki E, Not F, Mahé F. 2014. Intracellular diversity of the V4 and V9 regions of the 18S rRNA in marine protists (Radiolarians) assessed by high-throughput sequencing. *PLoS One* 9:e104297. <https://doi.org/10.1371/journal.pone.0104297>.
  19. Gong J, Dong J, Liu X, Massana R. 2013. Extremely high copy numbers and polymorphisms of the rDNA operon estimated from single cell analysis of oligotrich and peritrich ciliates. *Protist* 164:369–379. <https://doi.org/10.1016/j.protis.2012.11.006>.
  20. Kudryavtsev A, Gladkikh A. 2017. Two new species of *Ripella* (Amoebozoa, Vannellida) and unusual intragenomic variability in the SSU rRNA gene of this genus. *Eur J Protistol* 61:92–106. <https://doi.org/10.1016/j.ejop.2017.09.003>.
  21. Wang C, Zhang T, Wang Y, Katz LA, Gao F, Song W. 2017. Disentangling sources of variation in SSU rDNA sequences from single cell analyses of ciliates: impact of copy number variation and experimental error. *Proc R Soc B* 284:20170425. <https://doi.org/10.1098/rspb.2017.0425>.
  22. Gunderson JH, Sogin ML, Wollett G, Hollingdale M, de la Cruz VF, Waters AP, McCutchan TF. 1987. Structurally distinct, stage-specific ribosomes occur in *Plasmodium*. *Science* 238:933–937. <https://doi.org/10.1126/science.3672135>.
  23. López-López A, Benlloch S, Bonfá M, Rodríguez-Valera F, Mira A. 2007. Intra-genomic 16S rDNA divergence in *Haloarcula marismortui* is an adaptation to different temperatures. *J Mol Evol* 65:687–696. <https://doi.org/10.1007/s00239-007-9047-3>.
  24. Genuth NR, Barna M. 2018. The discovery of ribosome heterogeneity and its implications for gene regulation and organismal life. *Mol Cell* 71:364–374. <https://doi.org/10.1016/j.molcel.2018.07.018>.
  25. Kurylo CM, Parks MM, Juette MF, Zinshteyn B, Altman RB, Thibado JK, Vincent CT, Blanchard SC. 2018. Endogenous rRNA sequence variation can regulate stress response gene expression and phenotype. *Cell Rep* 25:236–248. <https://doi.org/10.1016/j.celrep.2018.08.093>.
  26. Prescott DM. 1994. The DNA of ciliated protozoa. *Microbiol Rev* 58:233–267. <https://doi.org/10.1128/mr.58.2.233-267.1994>.
  27. Postberg J, Alexandrova O, Lipps HJ. 2006. Synthesis of pre-rRNA and mRNA is directed to a chromatin-poor compartment in the macronucleus of the spirotrichous ciliate *Stylonychia lemnae*. *Chromosome Res* 14:161–175. <https://doi.org/10.1007/s10577-006-1033-x>.
  28. Gutiérrez JC, Martín-González A, Callejas S. 1998. Nuclear changes, macronuclear chromatin reorganization and DNA modifications during ciliate encystment. *Eur J Protistol* 34:97–103. [https://doi.org/10.1016/S0932-4739\(98\)80018-7](https://doi.org/10.1016/S0932-4739(98)80018-7).
  29. Zhao L, Li Y-S, Li J-G, Gu F-K. 2009. Some ultrastructural observations of the vegetative, resting and excysting ciliate, *urostylo grandis* (urostyliidae, hypotrichida). *Biol Res* 42:395–401. <https://doi.org/10.4067/s0716-97602009000400001>.
  30. Stout JD. 1955. Environmental factors affecting the life history of three soil species of *Colpoda* (Ciliata). *Trans R Soc New Zealand* 82:1165–1188.
  31. Müller H, Achilles-Day UEM, Day JG. 2010. Tolerance of the resting cysts of *Colpoda inflata* (Ciliophora, Colpodea) and *Meseres corlissi* (Ciliophora, Spirotrichea) to desiccation and freezing. *Eur J Protistol* 46:133–142. <https://doi.org/10.1016/j.ejop.2009.12.004>.
  32. Brown JH, Gillooly JF, Allen AP, Savage VM, West GB. 2004. Toward a metabolic theory of ecology. *Ecology* 85:1771–1789. <https://doi.org/10.1890/03-9000>.
  33. Engberg J, Pearlman RE. 1972. The amount of ribosomal RNA genes in *Tetrahymena pyriformis* in different physiological states. *Eur J Biochem* 26:393–400. <https://doi.org/10.1111/j.1432-1033.1972.tb01779.x>.
  34. Main CR, Doll C, Bianco C, Greenfield DI, Coyne KJ. 2014. Effects of growth phase, diel cycle and macronutrient stress on the quantification of *Heterosigma akashiwo* using qPCR and SHA. *Harmful Algae* 37:92–99. <https://doi.org/10.1016/j.hal.2014.05.014>.
  35. Galluzzi L, Bertozzini E, Penna A, Perini F, Garcés E, Magnani M. 2010. Analysis of rRNA gene content in the Mediterranean dinoflagellate *Alexandrium catenella* and *Alexandrium taylori*: implications for the quantitative real-time PCR-based monitoring methods. *J Appl Phycol* 22:1–9. <https://doi.org/10.1007/s10811-009-9411-3>.
  36. Eckford-Soper LK, Daugbjerg N. 2016. A quantitative real-time PCR assay for identification and enumeration of the occasionally co-occurring ichthyotoxic *Pseudochattonella farcimen* and *P. verruculosa* (Dictyochophyceae) and analysis of variation in gene copy numbers during the growth phase of single and mixed cultures. *J Phycol* 52:174–183. <https://doi.org/10.1111/jpy.12389>.
  37. Nishimura T, Hariganeya N, Tawong W, Sakanari H, Yamaguchi H, Adachi M. 2016. Quantitative PCR assay for detection and enumeration of ciguatera-causing dinoflagellate *Gambierdiscus* spp. in coastal areas of Japan. *Harmful Algae* 52:11–22. <https://doi.org/10.1016/j.hal.2015.11.018>.
  38. Corliss JO, Esser SC. 1974. Comments on the role of the cyst in the life cycle and survival of free-living protozoa. *Trans Am Microsc Soc* 93:578–593. <https://doi.org/10.2307/3225158>.
  39. Gillooly JF, Allen AP, Brown JH, Elser JJ, del Rio CM, Savage VM, West GB, Woodruff WH, Woods HA. 2005. The metabolic basis of whole-organism RNA and phosphorus content. *Proc Natl Acad Sci U S A* 102:11923–11927. <https://doi.org/10.1073/pnas.0504756102>.
  40. Weber AAT, Pawlowski J. 2013. Can abundance of protists be inferred from sequence data: a case study of Foraminifera. *PLoS One* 8:e56739. <https://doi.org/10.1371/journal.pone.0056739>.
  41. Wang Y, Wang C, Jiang Y, Katz LA, Gao F, Yan Y. 2019. Further analyses of variation of ribosome DNA copy number and polymorphism in ciliates provide insights relevant to studies of both molecular ecology and phylogeny. *Sci China Life Sci* 62:203–214. <https://doi.org/10.1007/s11427-018-9422-5>.
  42. Cavalier-Smith T. 1978. Nuclear volume control by nucleoskeletal DNA, selection for cell volume and cell growth rate, and the solution of the DNA C-value paradox. *J Cell Sci* 34:247–278. <https://doi.org/10.1242/jcs.34.1.247>.
  43. Atkinson D, Ciotti BJ, Montagnes DJS. 2003. Protists decrease in size linearly with temperature: ca. 2.5% °C<sup>-1</sup>. *Proc R Soc Lond B* 270:2605–2611. <https://doi.org/10.1098/rspb.2003.2538>.
  44. Elser JJ, Sterner RW, Gorokhova E, Fagan WF, Markow TA, Cotner JB, Harrison JF, Hobbie SE, Odell GM, Weider LW. 2000. Biological stoichiometry from genes to ecosystems. *Ecol Lett* 3:540–550. <https://doi.org/10.1111/j.1461-0248.2000.00185.x>.
  45. Weiss RL, Kukora JR, Adams J. 1975. The relationship between enzyme activity, cell geometry, and fitness in *Saccharomyces cerevisiae*. *Proc Natl Acad Sci U S A* 72:794–798. <https://doi.org/10.1073/pnas.72.3.794>.
  46. Mable BK, Otto SP. 2001. Masking and purging mutations following EMS treatment in haploid, diploid and tetraploid yeast (*Saccharomyces cerevisiae*). *Genet Res* 77:9–26. <https://doi.org/10.1017/s0016672300004821>.
  47. Hessen DO, Jeyasingh PD, Neiman M, Weider LJ. 2010. Genome streamlining and the elemental costs of growth. *Trends Ecol Evol* 25:75–80. <https://doi.org/10.1016/j.tree.2009.08.004>.
  48. Zhao F, Filker S, Xu K, Li J, Zhou T, Huang P. 2019. Effects of intragenomic polymorphism in the SSU rRNA gene on estimating marine microeukaryotic diversity: a test for ciliates using single-cell high-throughput DNA sequencing. *Limnol Oceanogr Methods* 17:533–543. <https://doi.org/10.1002/lom3.10330>.
  49. Alverson AJ, Kolnick L. 2005. Intra-genomic nucleotide polymorphism among small subunit (18S) rDNA paralogs in the diatom genus *Skeletonema*

- (Bacillariophyta). *J Phycol* 41:1248–1257. <https://doi.org/10.1111/j.1529-8817.2005.00136.x>.
50. Song W, Joo M, Yeom J-H, Shin E, Lee M, Choi H-K, Hwang J, Kim Y-I, Seo R, Lee JE, Moore CJ, Kim Y-H, Eyun S-I, Hahn Y, Bae J, Lee K. 2019. Divergent rRNAs as regulators of gene expression at the ribosome level. *Nat Microbiol* 4:515–526. <https://doi.org/10.1038/s41564-018-0341-1>.
  51. Benítez L, Gutiérrez JC. 1997. Encystment-specific mRNA is accumulated in the resting cysts of the ciliate *Colpoda inflata*. *Biochem Mol Biol Int* 41:1137–1141. <https://doi.org/10.1080/15216549700202221>.
  52. Palacios G, Martin-Gonzalez A, Gutierrez JC. 1994. Macronuclear DNA demethylation is involved in the encystment process of the ciliate *Colpoda inflata*. *Cell Biol Int* 18:201–206. <https://doi.org/10.1006/cbir.1994.1062>.
  53. Bernander R, Palm JED, Svård SG. 2001. Genome ploidy in different stages of the *Giardia lamblia* life cycle. *Cell Microbiol* 3:55–62. <https://doi.org/10.1046/j.1462-5822.2001.00094.x>.
  54. Mukherjee C, Clark CG, Lohia A. 2008. *Entamoeba* shows reversible variation in ploidy under different growth conditions and between life cycle phases. *PLoS Negl Trop Dis* 2:e281. <https://doi.org/10.1371/journal.pntd.0000281>.
  55. Cavalier-Smith T. 1980. r- and K-tactics in the evolution of protist developmental systems: cell and genome size, phenotype diversifying selection, and cell cycle patterns. *Biosystems* 12:43–59. [https://doi.org/10.1016/0303-2647\(80\)90037-4](https://doi.org/10.1016/0303-2647(80)90037-4).
  56. Omar A, Zhang Q, Zou S, Gong J. 2017. Morphology and phylogeny of the soil ciliate *Metopus yantaiensis* n. sp. (Ciliophora, Metopida), with identification of the intracellular bacteria. *J Eukaryot Microbiol* 64:792–805. <https://doi.org/10.1111/jeu.12411>.
  57. Wilbert N. 1975. Eine verbesserte technik der protargo-limpragnation fur ciliaten. *Mikrokosmos* 64:171–179.
  58. Gong J, Qing Y, Guo X, Warren A. 2014. “*Candidatus* Sonnebornia yantaiensis”, a member of candidate division OD1, as intracellular bacteria of the ciliated protist *Paramecium bursaria* (Ciliophora, Oligohymenophorea). *Syst Appl Microbiol* 37:35–41. <https://doi.org/10.1016/j.syapm.2013.08.007>.
  59. Zhu F, Massana R, Not F, Marie D, Vaulot D. 2005. Mapping of picoeucaryotes in marine ecosystems with quantitative PCR of the 18S rRNA gene. *FEMS Microbiol Ecol* 52:79–92. <https://doi.org/10.1016/j.femsec.2004.10.006>.
  60. Stoeck T, Bass D, Nebel M, Christen R, Jones MDM, Breiner H-W, Richards TA. 2010. Multiple marker parallel tag environmental DNA sequencing reveals a highly complex eukaryotic community in marine anoxic water. *Mol Ecol* 19:21–31. <https://doi.org/10.1111/j.1365-294X.2009.04480.x>.
  61. Díez B, Pedrós-Alió C, Marsh TL, Massana R. 2001. Application of denaturing gradient gel electrophoresis (DGGE) to study the diversity of marine picoeukaryotic assemblages and comparison of DGGE with other molecular techniques. *Appl Environ Microbiol* 67:2942–2951. <https://doi.org/10.1128/AEM.67.7.2942-2951.2001>.
  62. Dawson SC, Pace NR. 2002. Novel kingdom-level eukaryotic diversity in anoxic environments. *Proc Natl Acad Sci U S A* 99:8324–8329. <https://doi.org/10.1073/pnas.062169599>.
  63. Martin M. 2011. Cutadapt removes adapter sequences from high-throughput sequencing reads. *EMBnet J* 17:3. <https://doi.org/10.14806/ej.17.1.200>.
  64. Callahan BJ, McMurdie PJ, Rosen MJ, Han AW, Johnson AJA, Holmes SP. 2016. DADA2: High-resolution sample inference from Illumina amplicon data. *Nat Methods* 13:581–583. <https://doi.org/10.1038/nmeth.3869>.
  65. R Core Team. 2018. R: A language and environment for statistical computing. R Foundation for Statistical Computing, Vienna. <https://www.R-project.org>.
  66. Murali A, Bhargava A, Wright ES. 2018. IDTAXA: a novel approach for accurate taxonomic classification of microbiome sequences. *Microbiome* 6:140. <https://doi.org/10.1186/s40168-018-0521-5>.